

WL-TR-94-2034

LASER SPECTROSCOPY OF COMBUSTION  
INTERMEDIATES IN A SUPERSONIC JET EXPANSION

AD-A283 201



TORY

DR PRABHAKAR MISRA

HOWARD UNIVERSITY  
DEPT OF PHYSICS & ASTRONOMY  
WASHINGTON, DC 20059

MARCH 1994

FINAL REPORT FOR 04/30/90-03/31/94

APPROVED FOR PUBLIC RELEASE; DISTRIBUTION IS UNLIMITED.



528

94-25455



AEROPROPULSION AND POWER DIRECTORATE  
WRIGHT LABORATORY  
AIR FORCE MATERIEL COMMAND  
WRIGHT PATTERSON AFB OH 45433-7650

94 8 11 1 13

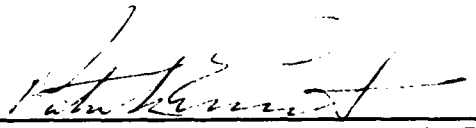
DTIC NUMBER 94-25455

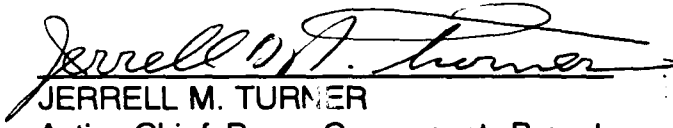
## NOTICE

When Government drawings, specifications, or other data are used for any purpose other than in connection with a definitely Government-related procurement, the United States Government incurs no responsibility or any obligation whatsoever. The fact that the government may have formulated or in any way supplied the said drawings, specifications, or other data, is not to be regarded by implication, or otherwise in any manner construed, as licensing the holder, or any other person or corporation; or as conveying any rights or permission to manufacture, use, or sell any patented invention that may in any way be related thereto.

This report is releasable to the National Technical Information Service (NTIS). At NTIS, it will be available to the general public, including foreign nations.

This technical report has been reviewed and is approved for publication.

  
PATRICK R. EMMERT, Capt, USAF  
Advanced Plasma Research Section  
Power Components Branch  
Aerospace Power Division  
Aero Propulsion and Power Directorate

  
JERRELL M. TURNER  
Acting Chief, Power Components Branch  
Aerospace Power Division  
Aero Propulsion and Power Directorate

  
MICHAEL D. BRAYDON

If your address has changed, if you wish to be removed from our mailing list, or if the addressee is no longer employed by your organization please notify WL/POOC, WPAFB, OH 45433-7919 to help us maintain a current mailing list.

Copies of this report should not be returned unless return is required by security considerations, contractual obligations, or notice on a specific document.

REPORT DOCUMENTATION PAGE			Form Approved OMB No. 0704-0188	
<small>Public reporting burden for this collection of information is estimated to average 1 hour per response, including the time for reviewing instructions, searching existing data sources, gathering and maintaining the data needed, and completing and reviewing the collection of information. Send comments regarding this burden estimate or any other aspect of this collection of information, including suggestions for reducing this burden, to Washington Headquarters Services, Directorate for Information Operations and Reports, 1215 Jefferson Davis Highway, Suite 1204, Arlington, VA 22202-4302, and to the Office of Management and Budget, Paperwork Reduction Project (0704-0188), Washington, DC 20503.</small>				
1. AGENCY USE ONLY (Leave blank)		2. REPORT DATE March 1994		3. REPORT TYPE AND DATES COVERED Final (30 April 90 - 31 March 94)
4. TITLE AND SUBTITLE Laser Spectroscopy of Combustion Intermediates in a Supersonic Jet Expansion.			5. FUNDING NUMBERS F33615-90-C-2038 PE: 62204 PR: 2003 TA: 12 WU: 08	
6. AUTHOR(S) Dr. Prabhakar Misra				
7. PERFORMING ORGANIZATION NAME(S) AND ADDRESS(ES) Howard University Department of Physics & Astronomy Washington, DC 20059			8. PERFORMING ORGANIZATION REPORT NUMBER	
9. SPONSORING/MONITORING AGENCY NAME(S) AND ADDRESS(ES) Aeropropulsion & Power Directorate Wright Laboratory Air Force Materiel Command Attn: Capt. Patrick Emmert Wright Patterson AFB, OH 45433-7650			10. SPONSORING/MONITORING AGENCY REPORT NUMBER  WL-TR-94-2034	
11. SUPPLEMENTARY NOTES				
12a. DISTRIBUTION/AVAILABILITY STATEMENT Approved for public release; distribution is unlimited.			12b. DISTRIBUTION CODE	
13. ABSTRACT (Maximum 200 words)  A detailed analysis of the laser-induced fluorescence spectra of jet-cooled alkoxy, alkylthio and aromatic radicals has helped to characterize these radicals spectroscopically. All three groups of radicals are involved in the chemistry of organic fuel combustion. A clearer knowledge about the spectroscopy of these chemical intermediates is necessary for improved understanding of the free-radical controlled reaction steps occurring in combustion processes.				
14. SUBJECT TERMS Spectroscopy; Combustion; Intermediates; Supersonic Jet			15. NUMBER OF PAGES 52	
			16. PRICE CODE	
17. SECURITY CLASSIFICATION OF REPORT UNCLASSIFIED	18. SECURITY CLASSIFICATION OF THIS PAGE UNCLASSIFIED	19. SECURITY CLASSIFICATION OF ABSTRACT UNCLASSIFIED	20. LIMITATION OF ABSTRACT UL	

## Table of Contents

List of Figures	iv
List of Tables	vi
1. Introduction	1
2. Experimental	3
3. Results and Discussion	9
4. References	41
5. Research Presentations and Publications	43

<b>Accession For</b>	
NTIS GRA&I	<input checked="" type="checkbox"/>
DTIC TAB	<input type="checkbox"/>
Unannounced	<input type="checkbox"/>
Justification	
By	
Distribution/	
<b>Availability Codes</b>	
Dist	Avail and/or Special
A-1	

## List of Figures

1. Experimental arrangement using an Nd:YAG-pumped dye laser for recording laser excitation spectra of jet-cooled free radicals. 4
2. Experimental arrangement using an excimer-pumped dye laser for recording laser excitation spectra of jet-cooled free radicals. 5
3. Experimental set-up to break Dicyclopentadiene. 6
4. Experimental arrangement for the laser optogalvanic (OG) effect. 7
5. Laser excitation spectrum of  $\text{CH}_3\text{O}$  showing  $3^2_0$  and  $2^1_0$  bands. The helium backing pressure was 120 psi and the time delay between the photolysis and probe lasers was 10  $\mu\text{s}$ . 10
6. Laser excitation scans showing the  $3^3_0$  and  $2^1_0 3^1_0$  bands of  $\text{CH}_3\text{O}$  obtained with 120 psi helium backing pressure for three separate time delays of 4.5, 6.5, 8.0  $\mu\text{s}$ , respectively, between the photolysis and probe lasers. 11
7. High resolution LIF excitation spectrum of the  $\tilde{A} - \tilde{X} 2^1_0$  band of the jet-cooled  $\text{CH}_3\text{O}$  radical showing assigned rotational transitions in the 32957-32967  $\text{cm}^{-1}$  spectral region. 16
8. High resolution (0.07  $\text{cm}^{-1}$ ) LIF excitation spectrum of the  $\tilde{A} - \tilde{X} 2^1_0 3^1_0$  band of  $\text{CH}_3\text{O}$  showing assigned rotational transitions. A backing pressure of 250 psi for the helium and methyl nitrite mixture was maintained behind the pulsed nozzle. 18
9. Laser-excited dispersed fluorescence spectrum of  $\text{CH}_3\text{O}$  observed when the  $2^1_0 3^1_0$  combination band was excited. 19
10. Rotationally-resolved LIF excitation spectrum of the  $\tilde{A} - \tilde{X} 9^4_0$  band of jet-cooled  $\text{C}_2\text{H}_5\text{O}$ . A He-backing pressure of 250 psi and a time delay of 8  $\mu\text{s}$  between the photolysis & probe lasers were used to obtain the spectrum. The dye DCM was used in the Nd:YAG-pumped dye laser to generate the probe beam of energy 0.2 mJ/pulse. 22
11. High resolution (0.07  $\text{cm}^{-1}$ ) rotationally-resolved laser excitation spectrum of the  $\tilde{A} - \tilde{X}$  band ( $\nu_0 = 27383.3 \text{ cm}^{-1}$ ) of jet-cooled  $i\text{-C}_3\text{H}_7\text{O}$ . The photolysis beam was a KrF laser (@248 nm) with an average energy of about 100 mJ/pulse. An excimer-pumped tunable laser with dye BPBD was used to generate a probe beam of about 1 mJ/pulse to record the spectrum. 25

12. Laser excitation scans showing the 26511-26533  $\text{cm}^{-1}$  spectral region for  $\text{CH}_3\text{S}$  obtained with 200 psi helium backing pressure for three separate time delays of 4  $\mu\text{s}$ , 6  $\mu\text{s}$ , and 8  $\mu\text{s}$ , respectively, between the photolysis and probe lasers. 28
  
13. (a) High resolution (0.07  $\text{cm}^{-1}$ ) LIF excitation spectrum of the  $\tilde{\text{A}} - \tilde{\text{X}}$   $0^0_0$  band of jet-cooled  $\text{CH}_3\text{S}$ . A backing pressure of 200 psi for the helium and  $(\text{CH}_3)_2\text{S}_2$  mixture was maintained behind the pulsed nozzle. (b) A trace showing the optogalvanic neon transition at 26515.07  $\text{cm}^{-1}$  and simultaneously recorded etalon fringes. 28
  
14. Laser-excited wavelength-resolved emission spectrum of  $\text{CH}_3\text{S}$  observed when the  $0^0_0$  band was pumped. Two series of progressions were seen and correspond to  $\tilde{\text{A}}^2\text{A}_1 - \tilde{\text{X}}^2\text{E}_{3/2}$  and  $\tilde{\text{A}}^2\text{A}_1 - \tilde{\text{X}}^2\text{E}_{1/2}$  transitions, respectively. 30
  
15. High resolution (0.07  $\text{cm}^{-1}$ ) rotationally-resolved laser excitation spectrum of the  $\tilde{\text{A}} - \tilde{\text{X}}$  band ( $\nu_0 = 25103.9 \text{ cm}^{-1}$ ) of jet-cooled  $\text{C}_2\text{H}_5\text{S}$ . The photolysis beam was a KrF laser (@248 nm) with an average energy of about 150 mJ/pulse. An excimer-pumped tunable laser with dye Ex 398 was used to generate a probe beam of about 2 mJ/pulse to record the spectrum. 33
  
16. High resolution (0.07  $\text{cm}^{-1}$ ) rotationally-resolved laser excitation spectrum of the  $\tilde{\text{A}} - \tilde{\text{X}}$  band ( $\nu_0 = 24773.7 \text{ cm}^{-1}$ ) of jet-cooled  $i\text{-C}_3\text{H}_7\text{S}$ . The photolysis beam was a KrF laser (@248 nm) with an average energy of about 100 mJ/pulse. An excimer-pumped tunable laser with dye DPS was used to generate a probe beam of about 1.5 mJ/pulse to record the spectrum. 36
  
17. LIF excitation spectrum of the  $\tilde{\text{A}}^2\text{A}_2'' - \tilde{\text{X}}^2\text{E}_1 0^0_0$  band of  $\text{C}_5\text{H}_5$ . 39
  
18. Laser excitation spectrum of benzyl showing various vibronic bands belonging to the  $\tilde{\text{A}}^2\text{A}_2 - \tilde{\text{X}}^2\text{B}_2$  electronic system. A backing pressure of 200 psi helium was maintained behind the nozzle and there was a time delay of 8  $\mu\text{s}$  between the photolysis and probe lasers. 40
  
19. Laser excitation scan showing the 22900-22980  $\text{cm}^{-1}$  spectral region for phenyl obtained with 200 psi helium backing pressure and a time delay of 6.5  $\mu\text{s}$  between the photolysis and probe lasers. The excimer-pumped dye laser with C440 dye had an average energy of 2 mJ per pulse. 40

## List of Tables

1.	Molecular constants used in the non-linear least-squares fit of the $\tilde{A}^2A_1 - \tilde{X}^2E$ rotational transitions for $CH_3O$ & $CH_3S$ .	13
2.	Band origins & upper state ( $\tilde{A}^2A_1$ ) and ground state ( $\tilde{X}^2E$ ) molecular constants (in $cm^{-1}$ ) for methoxy ( $CH_3O$ ) radical.	14
3.	Rotational transition frequencies of the ( $\tilde{A}^2A_1 - \tilde{X}^2E$ ) $2^1_0$ band of $CH_3O$ with the corresponding (J,K) assignments.	15
4.	Upper state ( $\tilde{A}^2A_1$ ) molecular constants and band origins (in $cm^{-1}$ ) for methoxy ( $CH_3O$ ) radical.	17
5.	Vibrational assignments of the intervals observed in dispersed fluorescence of $CH_3O \tilde{X}^2E$ . The numbers listed are differences between the pump frequency and the corresponding emission frequencies (in $cm^{-1}$ ).	20
6.	Rotational transition frequencies of the of the ( $\tilde{A} - \tilde{X}$ ) $9^4_0$ band of $C_2H_5O$ with corresponding prolate quantum number assignments.	23
7.	Molecular constants (in $cm^{-1}$ ) of the ethoxy ( $C_2H_5O$ ) radical.	24
8.	Rotational transition frequencies of the ( $\tilde{A} - \tilde{X}$ ) band ( $\nu_0=27383.3$ $cm^{-1}$ ) of isopropoxy ( $i-C_3H_7O$ ) with corresponding oblate quantum number assignments.	26
9.	Molecular constants (in $cm^{-1}$ ) of the isopropoxy ( $i-C_3H_7O$ ) radical.	27
10.	Band origins & upper state ( $\tilde{A}^2A_1$ ) and ground state ( $\tilde{X}^2E$ ) molecular constants (in $cm^{-1}$ ) for $CH_3S$ radical.	31
11.	Vibrational assignments of the intervals observed in dispersed fluorescence of $CH_3S \tilde{X}^2E$ . The numbers listed are differences between the pump frequency and the corresponding emission frequencies (in $cm^{-1}$ ).	32
12.	Rotational transition frequencies of the ( $\tilde{A} - \tilde{X}$ ) band ( $\nu_0=25103.9$ $cm^{-1}$ ) of $C_2H_5S$ with corresponding prolate quantum number assignments.	34

13. Molecular parameters (in  $\text{cm}^{-1}$ ) of alkylthio radicals. 35
14. Rotational transition frequencies of the of the ( $\tilde{A} - \tilde{X}$ ) band ( $\nu_0 = 24773.66 \text{ cm}^{-1}$ ) of  $i\text{-C}_3\text{H}_7\text{S}$  with corresponding oblate quantum number assignments. 37



## 1. Introduction

Neutral free radicals occur as significant chemical intermediates in gas-phase combustion chemistry. Over the course of the past three decades, our understanding of organic free radicals has been considerably enhanced by the introduction of new and novel experimental techniques, such as infrared laser absorption, microwave absorption, resonantly-enhanced multiphoton ionization and laser-induced fluorescence.<sup>1</sup> During the past 10 years, the technique of laser-induced fluorescence (LIF), in conjunction with a supersonic jet environment for the organic radicals,<sup>2</sup> has evolved into a dynamic area of investigation. In a typical LIF experiment, molecules are excited from ground electronic levels to excited electronic levels by the absorption of tunable laser radiation. Excited molecules can subsequently decay back to the ground electronic level, resulting in spontaneous emission or "fluorescence." By generating the organic radicals in a supersonic jet expansion, it is possible to study the molecules under very "cold" conditions. In a typical free jet expansion, the gas phase molecules can be produced with low vibrational temperatures ( $T_{\text{vib}} \sim 50$  K) and even lower rotational temperatures ( $T_{\text{rot}} \sim 5$  K) because of extensive cooling of the translational and internal degrees of freedom.<sup>3</sup> As a direct consequence of the cooling, even complex polyatomic organic molecules have only a few vibrational or rotational levels populated, whereby their spectra are simpler and readily interpretable. Such simplified spectra allow for a detailed spectroscopic characterization of moderate-sized organic radicals.

LIF is thus a powerful tool for the study of such jet-cooled polyatomic unstable molecular species. In contrast, owing to the fact that even moderately complex molecules have many quantum states populated at room temperature, traditional spectroscopic techniques would yield severely congested spectra that are often uninterpretable. Hence, a combination of the LIF method and the supersonic jet expansion provides an extremely sensitive and powerful technique for detection and detailed spectroscopic characterization of organic radicals.

The important difference in trying to probe highly reactive transient species as compared to relatively inert molecules in a jet is that the former cannot be seeded into the expansion gas reservoir, as these radicals would react with themselves, the reservoir walls or with impurities,<sup>4</sup> before they can traverse through the supersonic nozzle and be cooled by the expansion. Instead, these highly reactive chemical intermediates must be generated *in situ* in the jet expansion from suitable precursor molecules injected into the sample reservoir. This is accomplished by irradiating the precursor with photons from an excimer laser beam as they emanate from the nozzle orifice and travel downstream in the supersonic jet expansion.

We have applied the above ideas to understanding the basic molecular spectroscopy of certain jet-cooled organic radicals that are not well understood. For example, our spectroscopic knowledge about the alkoxy radicals ( $\text{RO}$ ;  $\text{R} = \text{CH}_3, \text{C}_2\text{H}_5, \text{i-C}_3\text{H}_7$ ), alkylthio radicals ( $\text{RS}$ ) and the aromatic radicals ( $\text{C}_5\text{H}_5, \text{C}_6\text{H}_5\text{CH}_2$  and  $\text{C}_6\text{H}_5$ ), is largely inadequate. Alkoxy radicals play a leading role as oxidation intermediates in the combustion of hydrocarbons and in air pollution.<sup>5</sup> Alkylthio radicals are involved in the chemistry of sulfur-rich fuels.<sup>6</sup> The aromatic radicals,

cyclopentadienyl ( $C_5H_5$ ), benzyl ( $C_6H_5CH_2$ ) and phenyl ( $C_6H_5$ ), are involved in soot formation associated with the burning of hydrocarbon fuels.<sup>7</sup>

The chemistry of organic fuel combustion invariably proceeds through a series of sequential reactions.<sup>8</sup> In almost all of such reactions, free radicals are key chemical intermediates.<sup>9</sup> Therefore, a clearer knowledge about the spectroscopy of these chemical intermediates would, in turn, lead to a greater understanding of the free radical-controlled reaction steps and thereby to improved and efficient combustion systems.

## 2. Experimental

The alkoxy (RO) radicals were generated *in situ* in the jet expansion by the excimer laser (KrF @ 248 nm or ArF @ 193 nm) photolysis of alkyl nitrites (RONO). The alkyl nitrites were synthesized by the dropwise addition of dilute sulfuric acid ( $\text{H}_2\text{SO}_4$ ) to a solution of sodium nitrite ( $\text{NaNO}_2$ ) and the corresponding alcohol (ROH).<sup>10</sup> The alkylthio (RS) radicals were produced by the excimer laser (248 or 193 nm radiation) photolysis of either the dialkyl sulfide ( $\text{R}_2\text{S}$ ) or the dialkyl disulfide ( $\text{R}_2\text{S}_2$ ). Both the sulfide precursors were available commercially (Aldrich or Sigma Chemical Co.). Figures 1 and 2 are schematic sketches of the two experimental arrangements (employing the Nd:YAG-pumped and excimer-pumped dye laser systems) that were used for recording the laser excitation spectra of the jet-cooled free radicals.

The cyclopentadiene ( $\text{C}_5\text{H}_6$ ) precursor for the cyclopentadienyl ( $\text{C}_5\text{H}_5$ ) radical is not available commercially. A glass manifold was designed and built (see Fig. 3) in order to facilitate breakage of the commercially available dicyclopentadiene dimer [ $(\text{C}_5\text{H}_6)_2$ ]. On heating the dimer to 160 °C, the cyclopentadiene ( $\text{C}_5\text{H}_6$ ) distilled smoothly (over a course of 4-5 hours). The  $\text{C}_5\text{H}_6$  precursor was placed in a stainless steel cylinder at room temperature prior to supersonic expansion. In order to produce the benzyl ( $\text{C}_6\text{H}_5\text{CH}_2$ ) radical, toluene ( $\text{C}_6\text{H}_5\text{CH}_3$ ) [or benzyl chloride ( $\text{C}_6\text{H}_5\text{CH}_2\text{Cl}$ )] was used as a precursor<sup>11</sup> together with 200 psi helium. Chlorobenzene ( $\text{C}_6\text{H}_5\text{Cl}$ ) and bromobenzene ( $\text{C}_6\text{H}_5\text{Br}$ ) were used as precursors<sup>12</sup> for the generation of jet-cooled phenyl ( $\text{C}_6\text{H}_5$ ) radical.

Each organic precursor was entrained in a flow of high-pressure (~10-14 atm) helium gas and the seeded flow was introduced into an expansion chamber through a commercial (General Valve) 0.5 mm pulsed nozzle. The radicals were formed by directing either a KrF or ArF excimer laser beam close to the expansion orifice so that the precursor molecules were effectively photolyzed. The photolyzed fragments were then probed by a pulsed tunable dye laser (either YAG- or excimer-pumped). Appropriate organic dyes were used in the dye laser circulator to cover the requisite wavelength range for laser excitation of the free radicals. A typical spatial separation of 10-12 mm was maintained between the photolysis and probe lasers. Laser-induced fluorescence from the excited radicals was collected by a quartz lens at right angles to the plane containing the counterpropagating laser beams and the supersonic nozzle (as shown in Figs. 1 and 2). The total fluorescence then impinged on a photomultiplier tube and the accumulated signals were averaged by a boxcar integrator (Stanford Research 250) in association with a microcomputer-aided data acquisition system. Laser excitation spectra of the jet-cooled free radicals were recorded by scanning the probe laser wavelength. The line-width afforded by the tunable dye laser pulse was about  $0.2\text{ cm}^{-1}$  and could be improved to  $0.05\text{-}0.07\text{ cm}^{-1}$ . Moderate resolution excitation spectra were used for vibronic assignments and the high resolution LIF spectra for rotational assignments.

Frequency calibration of the excitation spectra was accomplished by simultaneously recording either the absorption spectrum of iodine or the optogalvanic (OG) spectra of neon and argon. In case of OG calibration, a low-finesse reflection etalon provided an interference pattern that allowed interpolation between the identifiable OG transitions. The experimental arrangement

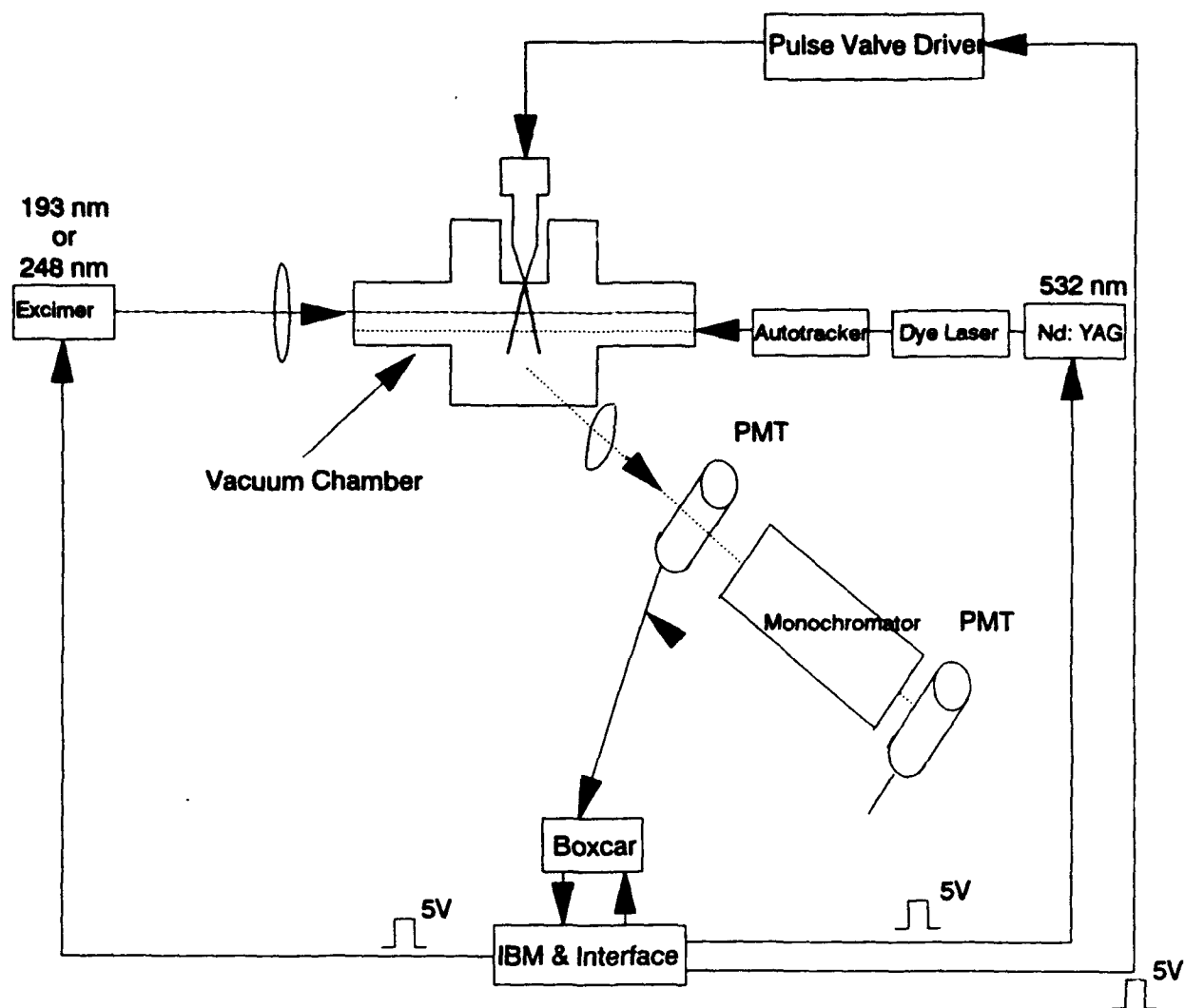
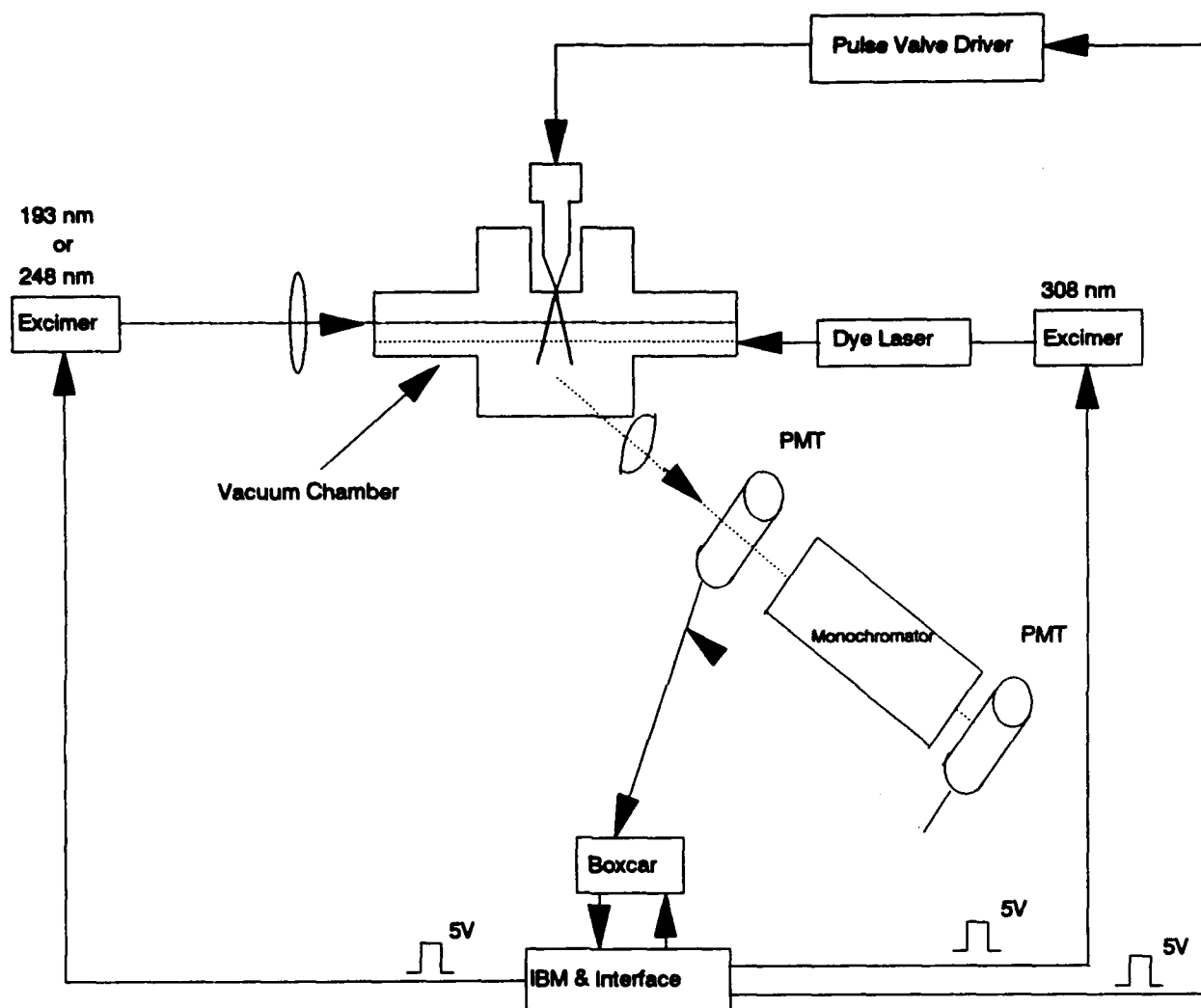
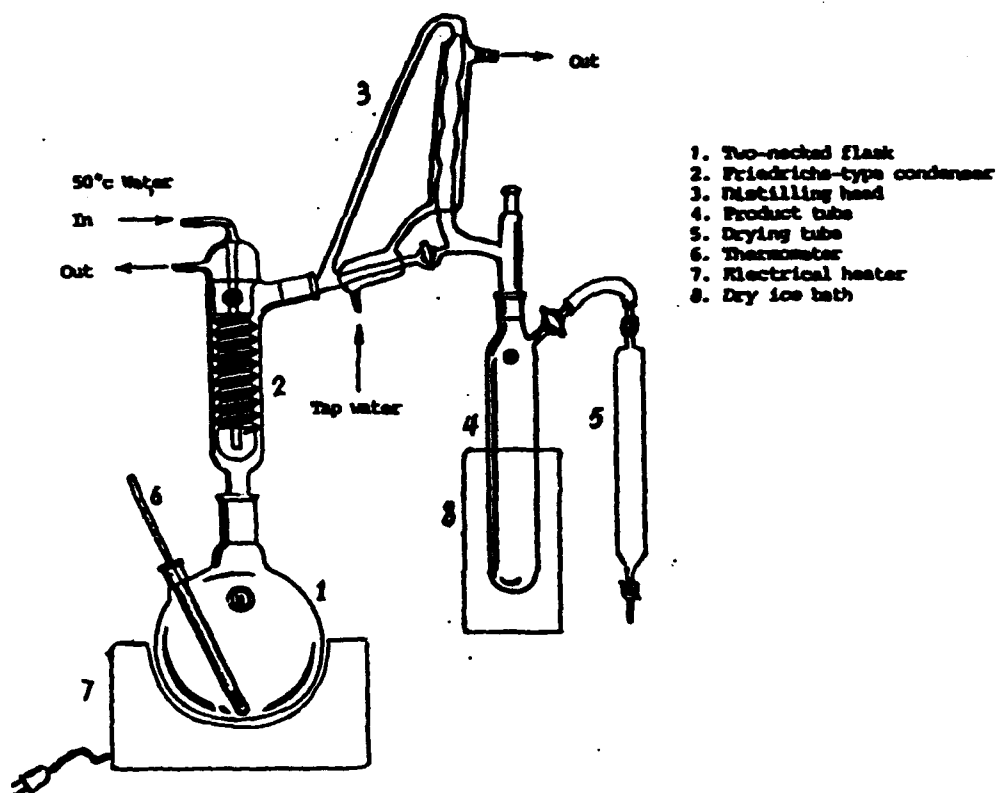


Figure 1: Experimental arrangement using an Nd:YAG-pumped dye laser for recording laser excitation spectra of jet-cooled free radicals.



**Figure 2: Experimental arrangement using an excimer-pumped dye laser for recording laser excitation spectra of jet-cooled free radicals.**



**Figure 3. Experimental set-Up to break Dicyclopentadiene**

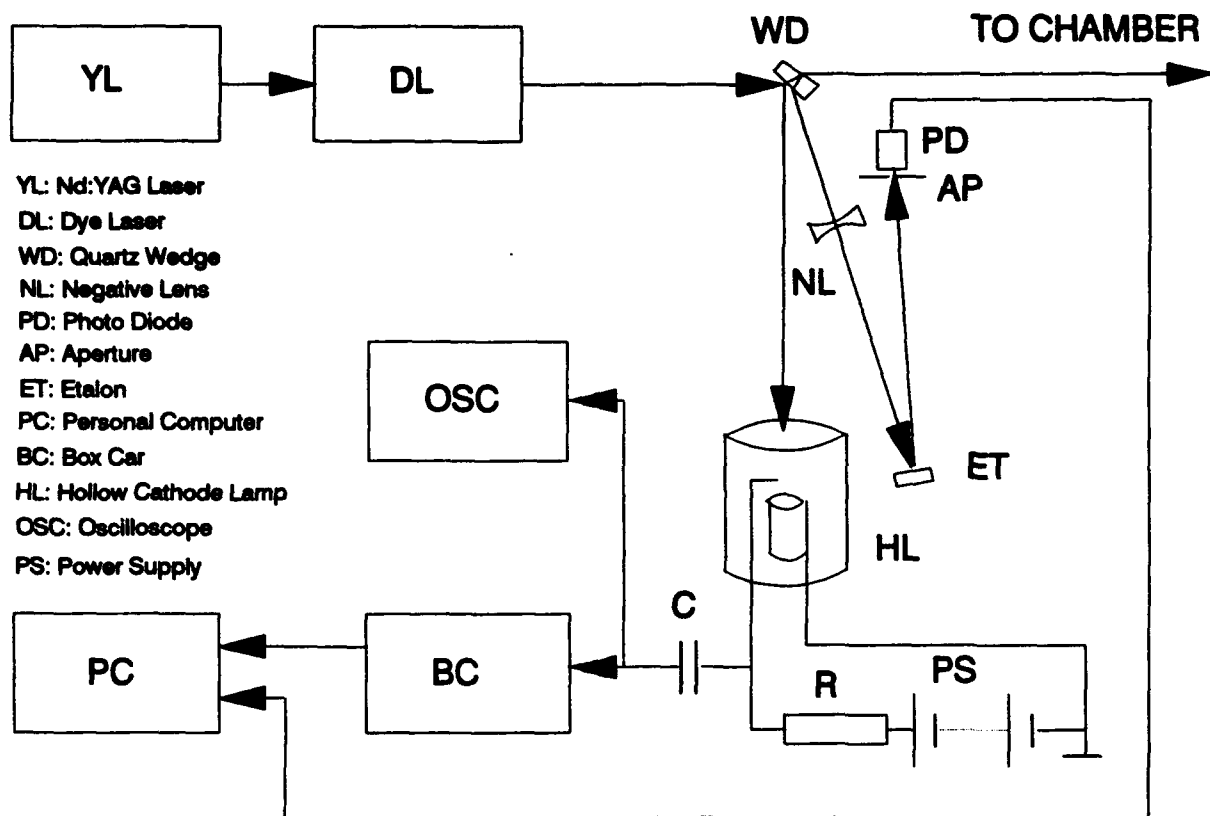


Figure 4: Experimental arrangement for the laser optogalvanic (OG) effect.

used for recording the OG transitions and the etalon fringes is shown in Fig. 4. An uncoated quartz wedge (WD) was inserted in the optical path of the dye laser beam in order to pick off two weak beams (each about 5% of the primary pulse energy). One of the beams (unfocused and of typical pulse energy 100  $\mu$ J) entered the cathode of a commercial iron-neon hollow cathode lamp (Perkin Elmer #303) through a 1 mm dia aperture. The second beam traversed a negative lens (NL) and illuminated an uncoated, parallel-faced 6 mm thick quartz disk at a small angle of incidence (1-2 deg) which served as a low-finesse etalon (ET) (see Fig. 4). The interference pattern - generated by the reflection beams from the front and rear surfaces of the disk - was recorded after passage through a pinhole aperture (AP) by a photodiode (PD). When the dye laser pulse was resonantly absorbed by the discharge medium, the voltage across the lamp varied, and these variations were coupled via a 0.05  $\mu$ F capacitor to a boxcar integrator (BC) (Stanford Research #520). Outputs of the boxcar and the photodiode were recorded simultaneously with a personal computer-aided data acquisition system.

Wavelength-resolved emission spectra of the  $\text{CH}_3\text{O}$  and  $\text{CH}_3\text{S}$  radicals were obtained by exciting the molecules at the wavelength of a rotational transition within a vibronic band. The total emitted fluorescence was focused onto the entrance slit of a 0.6 m monochromator (Jobin Yvon HRS 2) that provided a resolution of 0.3 nm. The output signal at the exit port was collected by a photomultiplier tube (as shown in Figs. 1 and 2) and processed by a microcomputer-aided data acquisition system. Dispersed fluorescence spectra recorded were analyzed to yield ground state vibrational frequencies and anharmonic parameters associated with the molecular potential energy.



### 3. Results and Discussion

#### Alkoxy Radicals

LIF excitation spectra of jet-cooled alkoxy ( $\text{RO}$ ,  $\text{R}=\text{CH}_3$ ,  $\text{C}_2\text{H}_5$ ,  $i\text{-C}_3\text{H}_7$ ) radicals have been recorded both under moderate ( $0.2\text{ cm}^{-1}$ ) and high ( $0.05\text{-}0.07\text{ cm}^{-1}$ ) resolution. Low resolution spectra have been used for vibronic assignments and the high resolution spectra for rotational assignments.

Figure 5 is an illustration of the  $32890\text{-}32990\text{ cm}^{-1}$  region of a typical LIF excitation spectrum of jet-cooled  $\text{CH}_3\text{O}$  obtained at a resolution of  $0.2\text{ cm}^{-1}$ . The backing pressure of the helium and methyl nitrite mixture behind the pulsed valve was 120 psi and the time delay between the photolysis and probe lasers was  $10\text{ }\mu\text{s}$ . Figure 5 shows the  $3^2_0$  band around  $32930\text{ cm}^{-1}$  and the  $2^1_0$  band in the vicinity of  $32960\text{ cm}^{-1}$ . Three scans for the  $3^3_0$  and  $2^1_0 3^1_0$  bands obtained with 120 psi backing pressure for three separate time delays of 4.5, 6.5 and  $8.0\text{ }\mu\text{s}$ , respectively, between the photolysis and probe lasers are shown in Fig. 6. An examination of the three scans in Fig. 6 clearly indicates the cooling effect realized in the supersonic jet expansion for longer time delays. Longer the time delay between the two lasers, the greater the number of collisions that the methoxy molecules suffer with the helium atoms comprising the carrier gas and lower the translational, vibrational and rotational temperatures in the jet expansion. For polyatomic molecules, like  $\text{CH}_3\text{O}$ , increased cooling results in perceptibly enhanced spectral resolution as is abundantly clear in the spectra displayed in Fig. 6.

$\text{CH}_3\text{O}$  is a prolate symmetric top molecule and has nominal  $\text{C}_{3v}$  symmetry. Its ground electronic state  $\tilde{\text{X}}^2\text{E}$  is doubly degenerate and subject to Jahn-Teller distortion.<sup>3</sup> The first excited electronic state of  $\text{CH}_3\text{O}$  is  $\tilde{\text{A}}^2\text{A}_1$ . The optical transition  $\tilde{\text{A}}^2\text{A}_1\text{-}\tilde{\text{X}}^2\text{E}$  in  $\text{CH}_3\text{O}$  occurs in the near UV. Rotationally-resolved  $\tilde{\text{A}}\text{-}\tilde{\text{X}}$  excitation spectra of  $\text{CH}_3\text{O}$  were recorded with a frequency-doubled scanning dye laser, while absorption spectra of molecular iodine were simultaneously recorded with the dye laser fundamental. An atlas<sup>13</sup> was used to identify the  $\text{I}_2$  transitions. Absolute wavenumbers for the rotational transitions involving the various vibronic  $\tilde{\text{A}}\text{-}\tilde{\text{X}}$  bands of  $\text{CH}_3\text{O}$  were generated by a non-linear least-squares fit using the  $\text{I}_2$  transitions belonging to the  $\text{B}^3\Pi^+_{\text{ou}}\text{-X}^1\Sigma^+$  electronic system in absorption. The rotational transitions for  $\text{CH}_3\text{O}$  have been assigned and labeled using the notation of Brown<sup>14</sup> and Herzberg.<sup>15</sup> The nomenclature employed for methoxy applies to prolate symmetric top transitions in doublet states. A primary symbol denotes the  $\Delta J$  character of the transition (P, Q and R for  $\Delta J = -1, 0$  and  $+1$ , respectively), while the superscript p or r differentiates  $\Delta K = -1$  from  $\Delta K = +1$  sub-bands. For a complete specification of a particular transition, it is necessary to label the  $\text{F}_1$  and  $\text{F}_2$  spin-rotation components that correspond to the values  $J = N + (1/2)$  and  $J = N - (1/2)$ , respectively. Thus, the subscripts attached to the transition symbol represent the  $\text{F}_1, \text{F}_2$  component character of the two rotational levels involved, the first subscript referring to the upper electronic state and the second to the lower electronic state. In all of the scans recorded for the  $\tilde{\text{A}}\text{-}\tilde{\text{X}}$  system of  $\text{CH}_3\text{O}$ , the spin-rotation doublet of the upper  $^2\text{A}_1$  state was unresolved and degenerate, whereby the transition frequency of  $\text{Q}(\text{J}, \text{K}, \text{F}_1)$  was the same as that of  $\text{P}(\text{J}, \text{K}, \text{F}_2)$  and the transition frequency of  $\text{R}(\text{J}, \text{K}, \text{F}_1)$  equalled that of  $\text{Q}(\text{J}, \text{K}, \text{F}_2)$ .<sup>3</sup> In such cases, only one of the two transitions involved

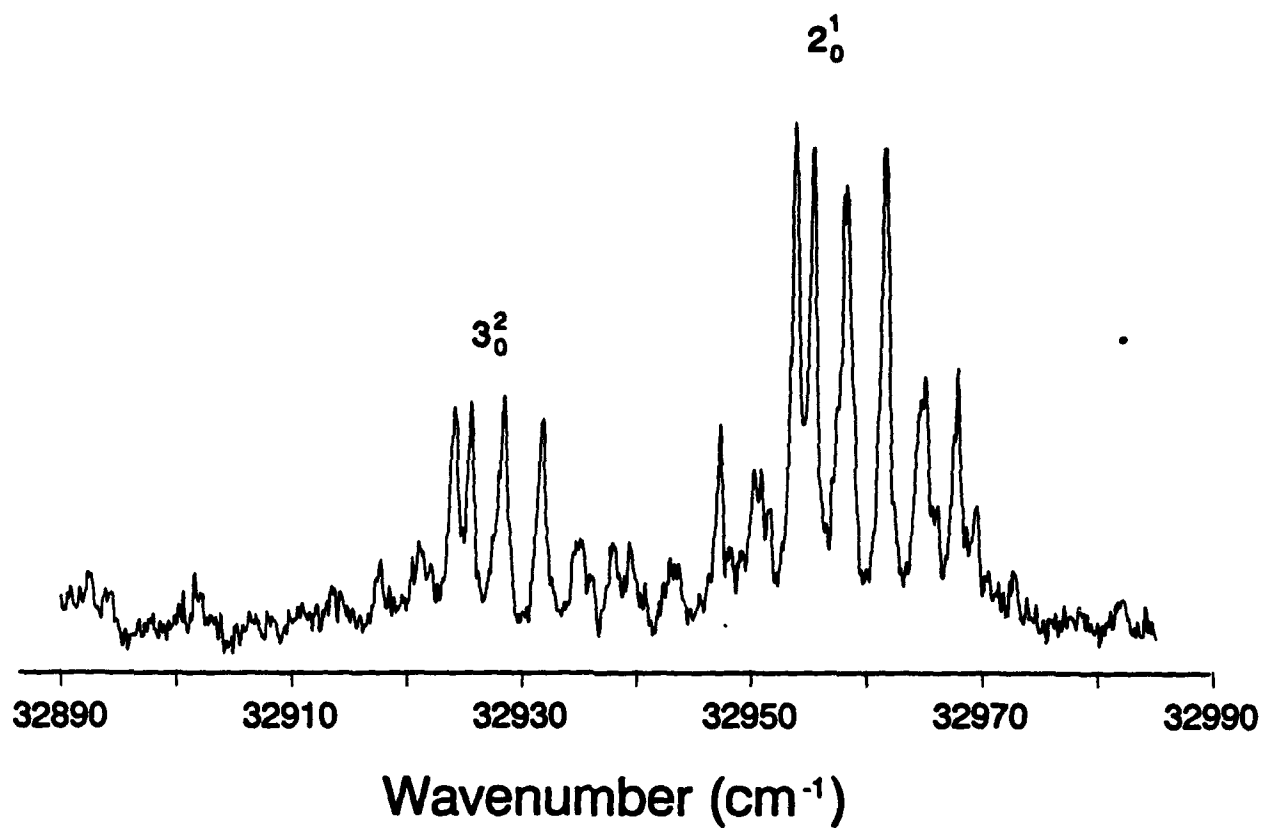
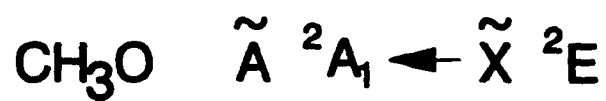


Figure 5. Laser excitation spectrum of  $\text{CH}_3\text{O}$  showing the  $3_0^2$  and  $2_0^1$  bands. The helium backing pressure was 120 psi and the time delay between the photolysis and probe lasers was  $10\mu\text{s}$ .

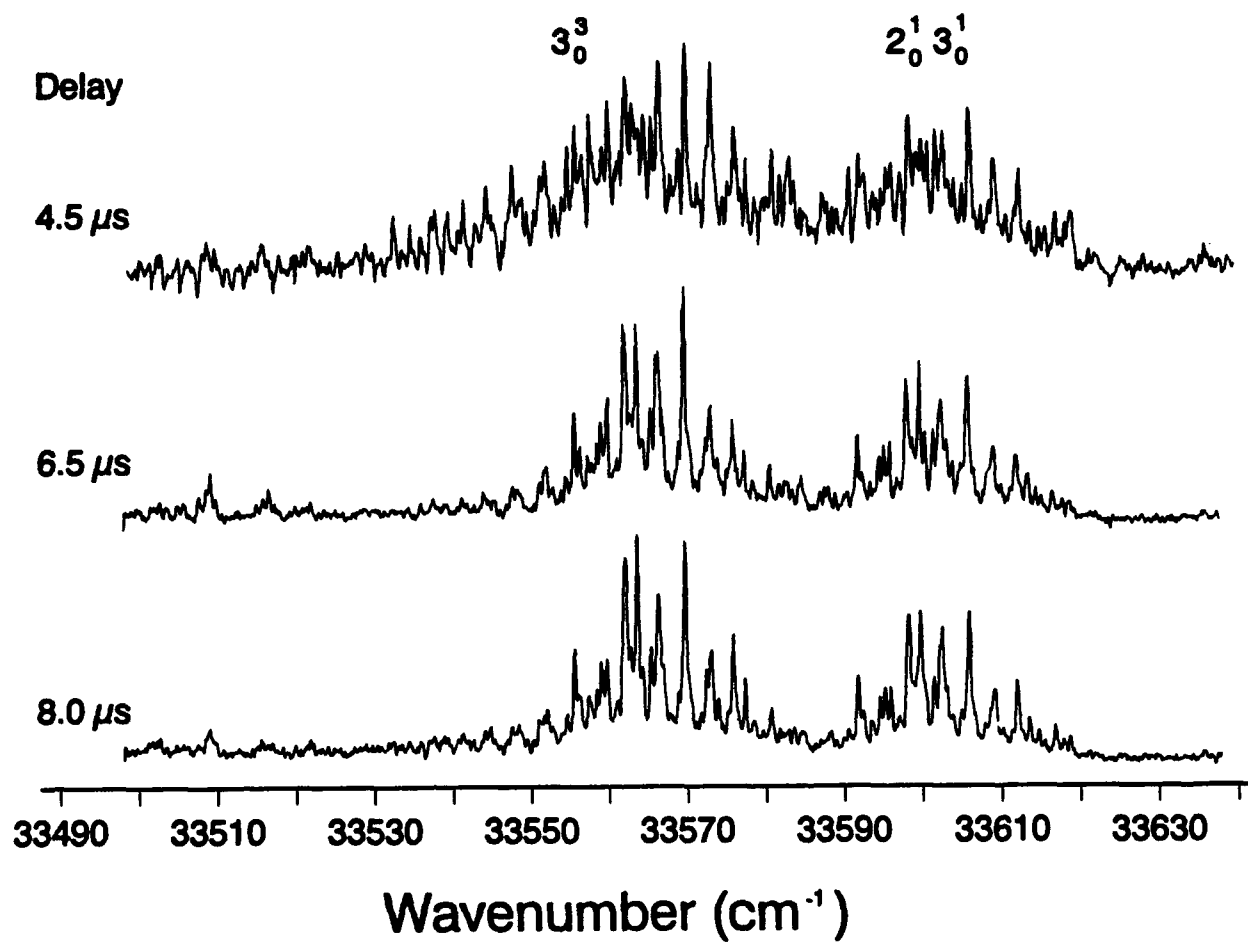
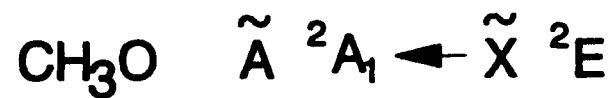


Figure 6: Laser excitation scans showing the  $3_0^3$  and  $2_0^1 3_0^1$  bands of  $\text{CH}_3\text{O}$  obtained with 120 psi helium backing pressure for three separate time delays of 4.5, 6.5 and 8.0  $\mu\text{s}$ , respectively, between the photolysis and probe lasers.

was identified and labeled.

Table 1 defines the molecular parameters used in the least-squares fits of the  $\tilde{A}^2A_1 - \tilde{X}^2E$  rotational transitions for the symmetric top molecule  $CH_3O$  (as well as  $CH_3S$ ) and Table 2 indicates the numerical ground ( $\tilde{X}^2E$ ) state constants of  $CH_3O$  fixed at the previously reported values in the literature.<sup>5</sup> The measured rotational transition frequencies for the  $\tilde{A}^2A_1 - \tilde{X}^2E$   $2^1_0$  band of  $CH_3O$  with the corresponding (J,K) assignments<sup>16</sup> are summarized in Table 3 and the transitions shown labeled explicitly in Fig. 7. The experimental uncertainty in the measured rotational line positions is estimated to be about  $0.10\text{ cm}^{-1}$ . Tables 2 and 4 summarize the upper state ( $\tilde{A}^2A_1$ ) molecular constants and the band origins for several  $CH_3O$  bands that were observed and analyzed. A rotationally-resolved laser excitation spectrum of the combination band  $\tilde{A} - \tilde{X} 2^1_0 3^1_0$  ( $\nu_0 = 33590.75\text{ cm}^{-1}$ ) of jet-cooled  $CH_3O$  is shown in Fig. 8. The upper state ( $\tilde{A}^2A_1$ ) rotational constants determined from the fit for the  $2^1_0 3^1_0$  band were  $A' = 4.99\text{ cm}^{-1}$  and  $B' = 0.73\text{ cm}^{-1}$ .

In order to derive information concerning the vibrational intervals in the ground state  $\tilde{X}^2E$  of  $CH_3O$ , the dye laser was tuned to the wavelength where the radical emitted the strongest fluorescence within a vibronic band. Single vibronic level dispersed fluorescence spectra<sup>17</sup> were then recorded for several methoxy bands by employing a monochromator that had an estimated resolution of  $0.3\text{ nm}$  with a slit-width of  $0.2\text{ mm}$ . An illustrative wavelength-resolved emission scan obtained by pumping the  $CH_3O$  combination band  $2^1_0 3^1_0$  is shown in Fig. 9. The first peak on the left of the spectrum corresponds to a mixture of the pump laser wavelength and the fluorescence due to the methoxy transition from the vibrational level in the excited state to that in the ground state. The  $\nu_3$  mode corresponding to the C-O symmetric stretch gives the strongest emission, and its "doubled progressions" are obvious; although the intensities of the members corresponding to the spin-orbit doublets vary. By doubled progressions is meant the consistent doubling of vibronic features in the dispersed spectrum - the doubling is a measure of the spin-orbit splitting ( $64\text{ cm}^{-1}$ ) of the methoxy ground state. The  $\nu_2$  emission is strong when the  $\nu_2$  mode (corresponding to the umbrella vibration) is pumped. Also, the  $\nu_5$  (scissor vibrational mode) and  $\nu_6$  (rocking mode) emissions are relatively stronger compared to those involving  $\nu_1$  ( $a_1$  C-H stretch) and  $\nu_4$  ( $e$  C-H stretch). All of the vibrational assignments for  $CH_3O$  are collected in Table 5.

**TABLE 1.**

**MOLECULAR CONSTANTS USED IN THE NON-LINEAR LEAST-SQUARES FIT  
OF THE  $\tilde{A}^2A_1 - \tilde{X}^2E$  ROTATIONAL TRANSITIONS FOR  $CH_3O$  &  $CH_3S$**

1. Rotational Constants for Lower State	$A' \text{ \& } B'$
2. Lower State Rovibronic Angular Momentum	$A'\xi_i$
3. Coriolis Centrifugal Distortion	$\eta_k\xi_i$
4. Spin Rotation Centrifugal Distortion	$\epsilon_{aa}, \epsilon_{bc}$
5. Spin-Orbital Coupling	$a\xi_e d$
6. Spin-Orbital Centrifugal Correction	$a_D\xi_e d$
7. Lower State Rotational Centrifugal Distortion	$D_a'', D_{ak}'', D_{a''}$
8. Centrifugal Correction of $A'\xi_i$	$\eta_e\xi_i$
9. Centrifugal Correction of Spin-Rotation	$\epsilon_{2a}, \epsilon_1$
10. Upper State Rotational Constants	$A' \text{ \& } B'$
11. Jahn-Teller Distortion Parameters	$h_1, h_{1N}, h_{1K}, h_2, h_{2N}, h_{2K}$
12. Upper State Rotational Centrifugal Distortion	$D_a', D_{ak}', D_k'$
13. Band Origin	$\nu_0$

TABLE 2.

Band Origins & Upper State ( $\tilde{A}^2A_1$ ) Molecular Constants (in  $\text{cm}^{-1}$ )  
for Methoxy ( $\text{CH}_3\text{O}$ ) Radical

Band	$3^3_0$		$2^1_0, 3^1_0$	
Parameter/ Constant	Initial Value	Final Value	Initial Value	Final Value
$A'$	4.9856	4.9660	4.9875	4.9530
$B'$	0.7374	0.7358	0.7732	0.7732
$\nu_0$	33551.88	33551.98	33588.40	33588.32
$D'_N$	$2.519 \times 10^{-06}{}^b$	$2.519 \times 10^{-06}$	$2.519 \times 10^{-06}{}^b$	$2.519 \times 10^{-06}$
$D'_{NK}$	$2.568 \times 10^{-05}{}^b$	$2.568 \times 10^{-05}$	$2.568 \times 10^{-05}{}^b$	$2.568 \times 10^{-05}$
$D'_K$	$7.030 \times 10^{-05}{}^b$	$7.030 \times 10^{-05}$	$7.030 \times 10^{-05}{}^b$	$7.030 \times 10^{-05}$

Ground State ( $\tilde{X}^2E$ ) Molecular Constants (in  $\text{cm}^{-1}$ )  
for Methoxy ( $\text{CH}_3\text{O}$ ) Radical

$A'$	5.2059	$\eta_e \xi_1$	$6.1 \times 10^{-05}$	$D'_N$	$2.519 \times 10^{-06}{}^b$
$B'$	0.9316825	$\epsilon_{2a}$	$8.092 \times 10^{-02}{}^a$	$D'_{NK}$	$2.568 \times 10^{-05}{}^b$
$A' \xi_1$	1.7730	$h_1$	$2.5117 \times 10^{-03}$	$D'_K$	$7.03 \times 10^{-05}{}^b$
$\eta_k \xi_1$	$4.400 \times 10^{-03}$	$h_{1N}$	0.0	$\epsilon_1$	$-5.7359 \times 10^{-03}$
$\epsilon_m$	-1.3533	$h_{1K}$	$7.86 \times 10^{-06}$		
$\epsilon_{bc}$	$-4.35 \times 10^{-02}$	$h_2$	$4.605 \times 10^{-02}$		
$a \xi_e d$	-61.974	$h_{2N}$	$-1.6 \times 10^{-07}$		
$a_D \xi_e d$	$3.56 \times 10^{-03}$	$h_{2K}$	$-1.81 \times 10^{-05}$		

<sup>a</sup>  $\epsilon_{2a} = \epsilon_{2a} \times B'/A'$

<sup>b</sup> also fixed for upper state.

TABLE 3.

Rotational Transition Frequencies of the ( $\tilde{A}^2A_1 - \tilde{X}^2E$ )  $2^1_0$  Band of  $\text{CH}_3\text{O}$   
with the Corresponding (J,K) Assignments

J'	K'	J <sub>1</sub> '	J <sub>2</sub> '	K'	Wavenumber (cm <sup>-1</sup> )	Obs-Cal	Transition
5.5	1.0	5.5	4.5	0.0	32958.26	-0.114	<sup>p</sup> Q <sub>11</sub> (5.5, 1.0)
2.5	2.0	1.5		1.0	32958.86	-0.089	<sup>p</sup> P <sub>11</sub> (2.5, 2.0)
3.5	2.0	3.5	2.5	1.0	32959.69	-0.255	<sup>p</sup> Q <sub>11</sub> (3.5, 2.0)
5.5	0.0	5.5	4.5	1.0	32961.73	-0.069	<sup>r</sup> Q <sub>11</sub> (5.5, 0.0)
2.5	2.0	2.5	1.5	1.0	32961.97	-0.087	<sup>p</sup> Q <sub>11</sub> (2.5, 2.0)
2.5	1.0	1.5		0.0	32962.58	0.126	<sup>p</sup> P <sub>11</sub> (2.5, 1.0)
3.5	1.0	3.5	2.5	0.0	32963.41	0.010	<sup>p</sup> Q <sub>11</sub> (3.5, 1.0)
5.5	2.0	6.5	5.5	1.0	32963.96	0.205	<sup>p</sup> R <sub>11</sub> (5.5, 2.0)
4.5	0.0	4.5	3.5	1.0	32964.39	-0.131	<sup>r</sup> Q <sub>11</sub> (4.5, 0.0)
2.5	1.0	2.5	1.5	0.0	32965.23	-0.120	<sup>p</sup> Q <sub>11</sub> (2.5, 1.0)
1.5	1.0	0.5		0.0	32965.48	0.005	<sup>p</sup> P <sub>11</sub> (1.5, 1.0)
2.5	0.0	1.5		1.0	32966.07	0.190	<sup>p</sup> P <sub>11</sub> (2.5, 0.0)
2.5	2.0	3.5	2.5	1.0	32966.36	0.077	<sup>p</sup> R <sub>11</sub> (2.5, 2.0)
3.5	0.0	3.5	2.5	1.0	32966.85	-0.005	<sup>r</sup> Q <sub>11</sub> (3.5, 0.0)
2.5	0.0	2.5	1.5	1.0	32968.92	0.106	<sup>r</sup> Q <sub>11</sub> (2.5, 0.0)
3.5	3.0		4.5	2.0	32969.59	-0.076	<sup>p</sup> R <sub>21</sub> (3.5, 3.0)
2.5	1.0	3.5	2.5	0.0	32969.74	-0.010	<sup>p</sup> R <sub>11</sub> (2.5, 1.0)
5.5	0.0	6.5	5.5	1.0	32970.66	0.062	<sup>r</sup> R <sub>11</sub> (5.5, 0.0)

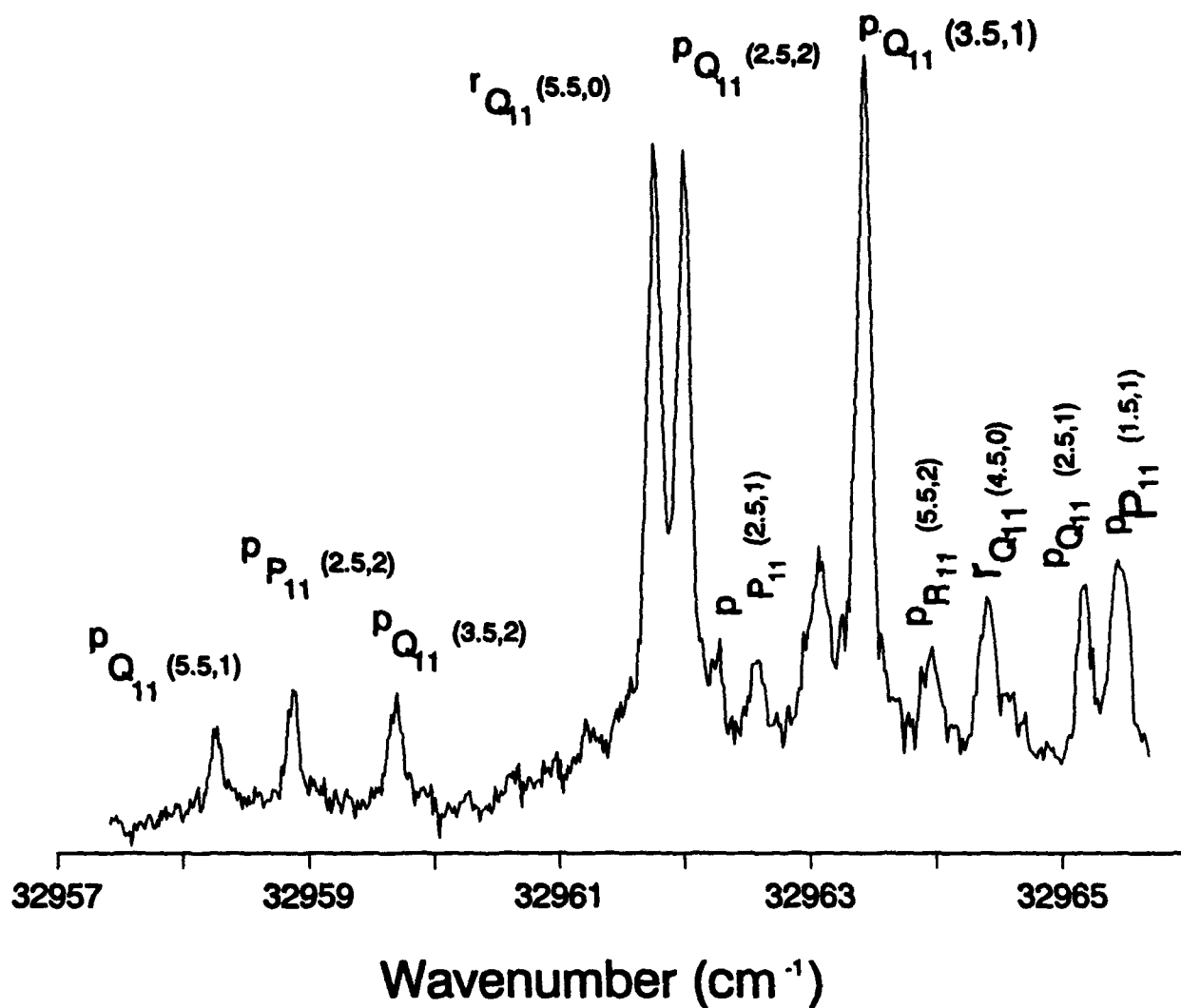
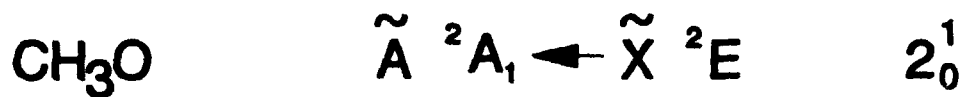


Figure 7: High resolution LIF excitation spectrum of the  $\tilde{A}-\tilde{X}^2_0^1$  band of the jet-cooled CH<sub>3</sub>O radical showing assigned rotational transitions in the 32957-32967 cm<sup>-1</sup> spectral region.



**TABLE 4.**

**Upper State ( $\tilde{A}^2A_1$ ) Molecular Constants and Band Origins (in  $\text{cm}^{-1}$ )  
for Methoxy ( $\text{CH}_3\text{O}$ ) Radical**

Constants	$0^0_0$	$3^1_0$	$2^1_0$	$2^1_0, 3^1_0$
$A'$	4.984	4.982	4.988	4.989
$B'$	0.743	0.731	0.750	0.733
$\nu_0$	31614.51	32276.87	32935.25	33590.75

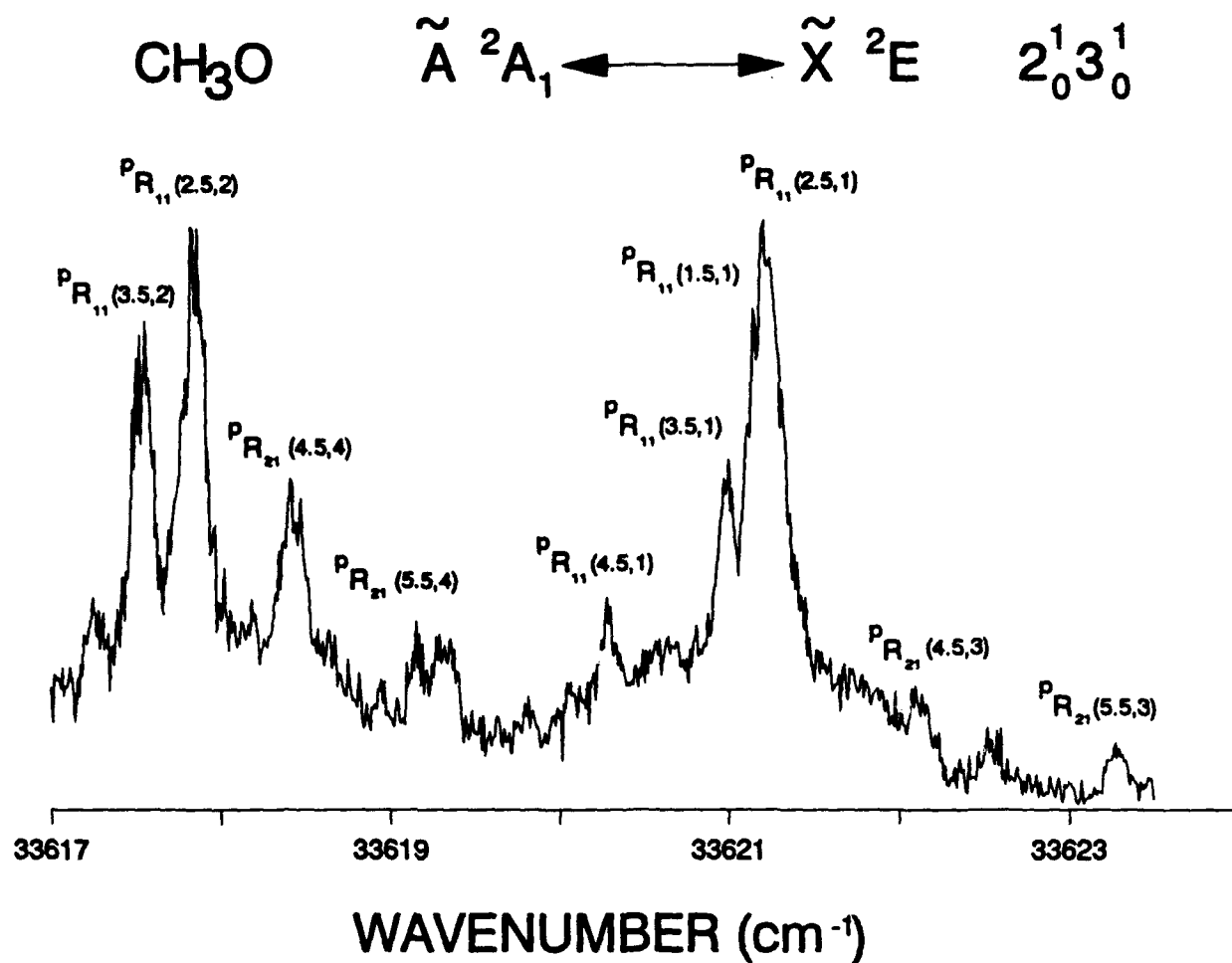


Figure 8: High resolution ( $0.07 \text{ cm}^{-1}$ ) LIF excitation spectrum of the  $\tilde{\text{A}}\text{-}\tilde{\text{X}} \ 2_0^1 3_0^1$  band of  $\text{CH}_3\text{O}$  showing assigned rotational transitions. A backing pressure of 250 psi for the helium and methyl nitrite mixture was maintained behind the pulsed nozzle.

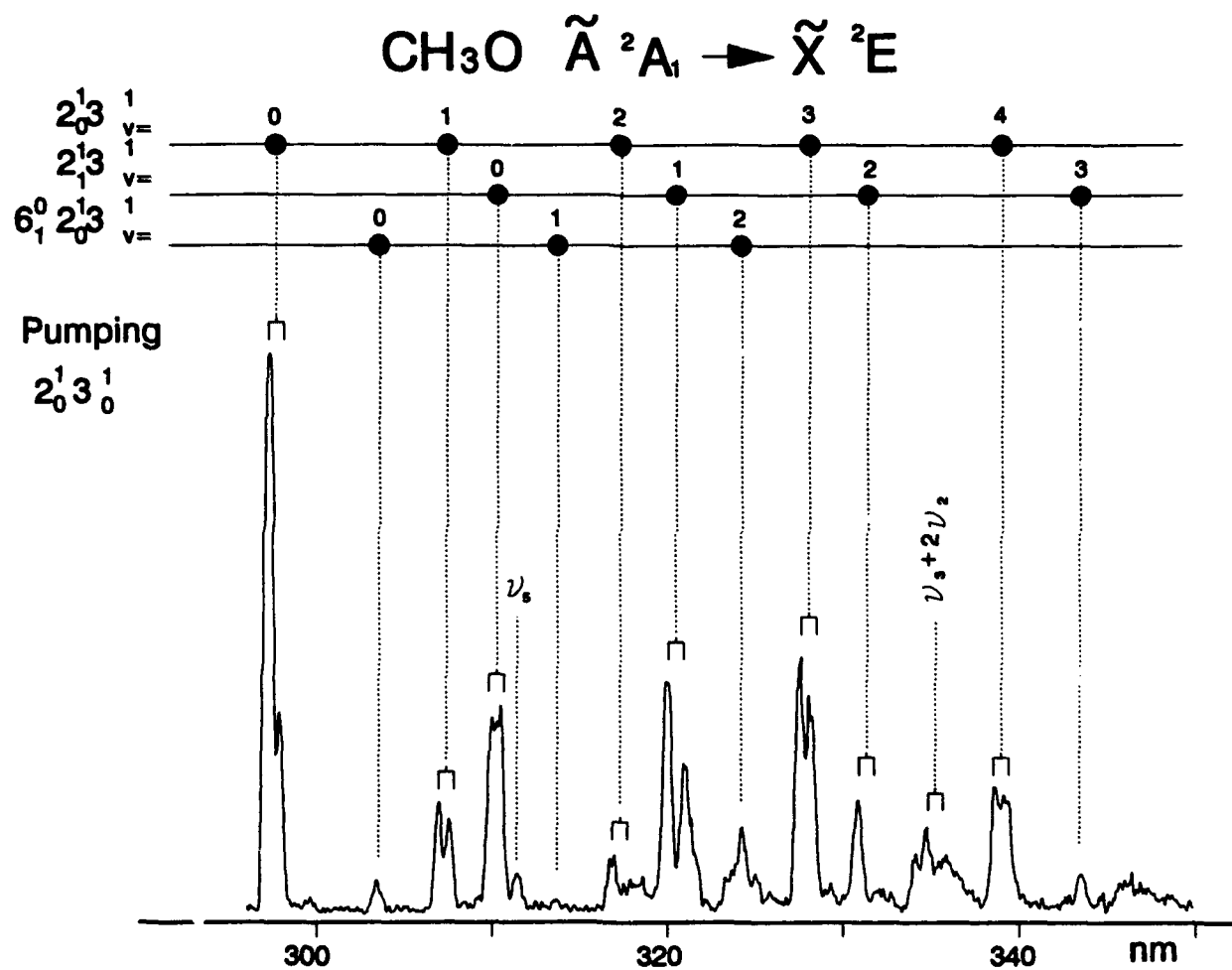


Figure 9: Laser-excited dispersed fluorescence spectrum of  $\text{CH}_3\text{O}$  observed when the  $2_0^1 3_1^1$  combination band was excited.

TABLE 5.

## Vibrational Assignments of the Intervals Observed in Dispersed Fluorescence

of  $\text{CH}_3\text{O } \tilde{\text{X}}^2\text{E}$ . The numbers listed are differences betweenthe pump frequency and the corresponding emission frequencies (in  $\text{cm}^{-1}$ ).

$\tilde{\text{A}}^2\text{A}_1-\tilde{\text{X}}^2\text{E}_{3/2}$	$\tilde{\text{A}}^2\text{A}_1-\tilde{\text{X}}^2\text{E}_{1/2}$	Assignment	$\tilde{\text{A}}^2\text{A}_1-\tilde{\text{X}}^2\text{E}_{3/2}$	$\tilde{\text{A}}^2\text{A}_1-\tilde{\text{X}}^2\text{E}_{1/2}$	Assignment
0	64		3413		$2\nu_2+\nu_6$
688		$\nu_6$		3518	$2\nu_3+\nu_2$
1062	1128	$\nu_3$	3560		$\nu_1+\nu_6$
1240		$2\nu_6$	3707		$\nu_4+\nu_6$
1375	1438	$\nu_2$	3770	3858	$\nu_3+2\nu_2$
1528		$\nu_5$	4112	4173	$4\nu_3$
1694		$3\nu_6$		4203	$\nu_2+2\nu_3+\nu_6$
1760		$\nu_3+\nu_6$		4306	$2\nu_2+\nu_5$
2084	2149	$2\nu_3$		4412	$3\nu_3+2\nu_6$
2247		$\nu_5+\nu_6$		4536	$3\nu_3+\nu_2$
	2386	$\nu_3+2\nu_6$		4740	$\nu_2+2\nu_3+2\nu_6$
	2484	$\nu_2+\nu_3$	4815	4905	$2\nu_3+2\nu_2$
2535		(?)	5101	5142	$5\nu_3$
2567		$\nu_3+\nu_5$		5428	$4\nu_3+2\nu_6$
2719	2796	$2\nu_2$		5536	$4\nu_3+\nu_2$
	2818	$2\nu_3+\nu_6$		5703	$4\nu_3+\nu_5$
2869	2953	$\nu_1$		5808	$5\nu_3+\nu_6$
3020		$\nu_4$		5931	$3\nu_3+2\nu_2$
3113	3160	$3\nu_3$	6089	6118	$6\nu_3$
	3269	$\nu_3+\nu_5+\nu_6$		6497	$5\nu_3+\nu_2$

High resolution LIF spectra of jet-cooled ethoxy ( $C_2H_5O$ ) and isopropoxy ( $i-C_3H_7O$ ) radicals were also recorded and analyzed. Molecular parameters characterizing the ground and excited electronic states have been obtained for both ethoxy and isopropoxy following a least-squares fit of the assigned rotational transitions.

$C_2H_5O$  shows a C-type perpendicular band structure<sup>15</sup> of a near prolate symmetric top molecule ( $k \geq 0.92$ ) as illustrated by the rotational structure of the  $9^4_0$  band displayed in Fig. 10. The  $\nu_9$  mode corresponds to the symmetric C-O stretch vibration. The electronic wavefunctions of  $C_2H_5O$  transform according to one of two irreducible representations of the  $C_2$  point group. Using the nomenclature developed by Herzberg<sup>15</sup> and Foster et al.,<sup>18</sup> the rotational structure exhibited by the  $9^4_0$  band of ethoxy is indicative of the electronic transition  $\tilde{A}^2A' - \tilde{X}^2A''$ . Table 6 summarizes the rotational assignments for the  $\tilde{A} - \tilde{X}^4_0$  band, together with residuals (Obs-Cal) that indicate the good quality of the fit. High resolution analysis employing prolate symmetric top quantum numbers for the  $\tilde{A} - \tilde{X}^4_0$  band of  $C_2H_5O$  yields:  $\nu_0 = 31558.11 \text{ cm}^{-1}$ ,  $A' = 1.14 \text{ cm}^{-1}$ ,  $B' = 0.30 \text{ cm}^{-1}$ ,  $C' = 0.29 \text{ cm}^{-1}$ ,  $A'' = 1.29 \text{ cm}^{-1}$ ,  $B'' = 0.31 \text{ cm}^{-1}$  and  $C'' = 0.29 \text{ cm}^{-1}$ ; and have been collected in Table 7. Table 7 also summarizes the upper and lower state rotational constants obtained by a fit we performed on the  $9^1_0$  band transitions reported by Foster et al.<sup>18</sup> For comparison, parameters recently calculated by Miller et al.<sup>19</sup> for the  $0^0_0$  and  $9^2_0$  bands of ethoxy have also been included in Table 7.

Isopropoxy has  $C_s$  symmetry<sup>15,18</sup> and is an oblate symmetric top molecule ( $k \geq 0.78$ ). Figure 11 is an illustration of the rotationally-resolved spectrum of a vibronic band of jet-cooled  $i-C_3H_7O$  in the vicinity of  $27,383 \text{ cm}^{-1}$ . The observed rotational structure mimics that of a parallel type band. However, Herzberg<sup>15</sup> forbids the observance of a parallel band for an isopropoxy-type molecule. Thus, we are forced to draw the conclusion - as corroborated by Foster et al.<sup>18</sup> - that we have observed the strong parallel component of a hybrid band, while the perpendicular component of the band is too weak to be recorded. Table 8 is a collection of the rotational transition frequencies for the  $\tilde{A} - \tilde{X}$  band ( $\nu_0 = 27,383.3 \text{ cm}^{-1}$ ) of  $i-C_3H_7O$  together with assigned oblate quantum numbers and separated  $K''$ -manifolds. The rotational parameters obtained for the upper state ( $A', B', C'$ ) and those for the lower state ( $A'', B'', C''$ ) of the  $\tilde{A} - \tilde{X}$  electronic system of  $i-C_3H_7O$  following a least-squares fit of the transitions have been collected in Table 9. For comparison, we have included in Table 9, the rotational constants obtained by a fit we performed on the  $0^0_0$  band transitions reported earlier in the literature.<sup>18</sup>

### Alkylthio Radicals

Figure 12 is an illustration showing three excitation scans for the methylthio ( $CH_3S$ ) radical in the wavenumber domain  $26511\text{--}26533 \text{ cm}^{-1}$  obtained with an excimer-pumped dye laser with an average energy of 2 mJ per pulse. A KrF photolysis excimer beam of 80 mJ per pulse photodissociated the  $(CH_3)_2S_2$  precursor. The backing pressure of the helium and disulfide mixture was maintained at 200 psi for three separate time delays of 4  $\mu\text{s}$ , 6  $\mu\text{s}$  and 8  $\mu\text{s}$ , respectively, between the photolysis and probe lasers. An examination of the composite scan shown in Fig. 12 reveals the cooling effect realized in the supersonic expansion for longer time

Ethoxy  
(C<sub>2</sub>H<sub>5</sub>O)



9<sub>0</sub><sup>4</sup>

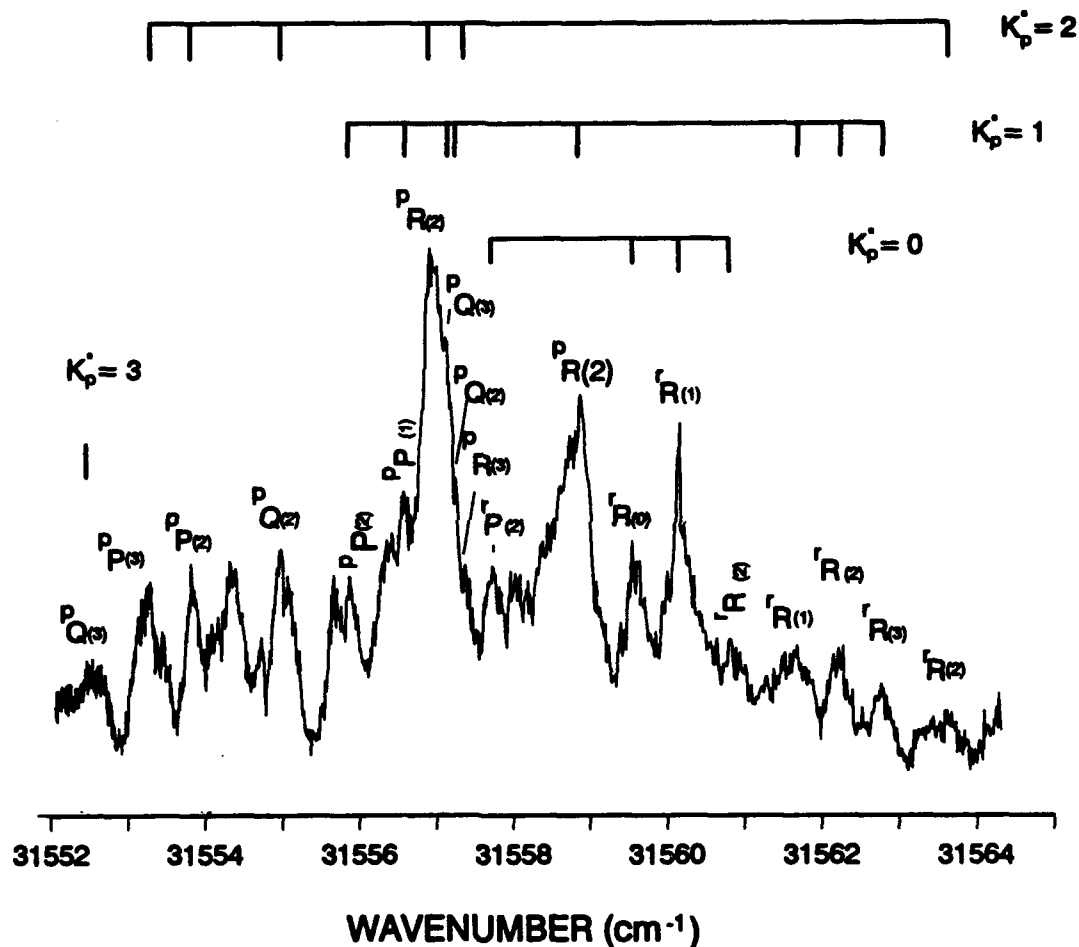


Figure 10. Rotationally-resolved LIF excitation spectrum of the  $\tilde{A}-\tilde{X}$  9<sub>0</sub><sup>4</sup> band of jet-cooled C<sub>2</sub>H<sub>5</sub>O. A He-backing pressure of 250 psi and a time delay of 8 μs between the photolysis & probe lasers were used to obtain the spectrum. The dye DCM was used in the Nd:YAG-pumped dye laser to generate the probe beam of energy 0.2 mJ/pulse.

TABLE 6.

Rotational Transition Frequencies of the ( $\tilde{A} - \tilde{X}$ )  $9^+_u$  Band of  $C_2H_5O$ 

with Corresponding Prolate Quantum Number Assignments

$J''$	$K''_u$	$J'$	$K'_u$	Wavenumber ( $cm^{-1}$ )	Obs-Cal	Transition
2	0	1	1	31557.69	-0.066	$^uP(2)$
0	0	1	1	31559.53	-0.044	$^uR(0)$
1	0	2	1	31560.14	-0.031	$^uR(1)$
2	0	3	1	31560.80	-0.037	$^uR(2)$
2	1	1	0	31555.85	-0.038	$^uP(2)$
1	1	0	0	31556.52	-0.007	$^uP(1)$
3	1	3	3	31557.09	-0.029	$^uQ(3)$
2	1	2	0	31557.22	0.088	$^uQ(2)$
2	1	3	0	31558.85	0.002	$^uR(2)$
1	1	2	2	31561.67	0.002	$^uR(1)$
2	1	3	2	31562.25	-0.022	$^uR(2)$
3	1	4	2	31562.76	0.021	$^uR(3)$
3	2	2	1	31553.27	0.086	$^uP(3)$
2	2	1	1	31553.80	0.017	$^uP(2)$
2	2	2	1	31554.97	0.020	$^uQ(2)$
2	2	3	2	31556.89	0.083	$^uR(2)$
3	2	4	1	31557.32	-0.073	$^uR(3)$
2	2	3	3	31563.51	0.029	$^uR(2)$
3	3	3	2	31552.44	-0.074	$^uQ(3)$

TABLE 7.

Molecular Constants (in  $\text{cm}^{-1}$ ) of the Ethoxy ( $\text{C}_2\text{H}_5\text{O}$ ) Radical

Constant	$0_0^0$ (Ref. 19)	$9_0^1$ (Ref. 18) <sup>a</sup>	$9_0^2$ (Ref. 19)	$9_0^4$ (Present Work)
A''	1.317	1.223	1.316	1.292
B''	0.320	0.310	0.320	0.313
C''	0.284	0.310	0.284	0.293
A'	1.116	1.100	1.134	1.137
B'	0.311	0.311	0.311	0.305
C'	0.267	0.274	0.271	0.287
$\nu_0$	29210.2	29783.8	30380.5	31558.1

<sup>a</sup> Rotational constants obtained by a fit we performed on the  $9_0^1$  band transitions reported in Ref. 18.



# Isopropoxy

(i-C<sub>3</sub>H<sub>7</sub>O)  $\tilde{A} \longleftarrow \tilde{X}$  Band at 27383.3 cm<sup>-1</sup>

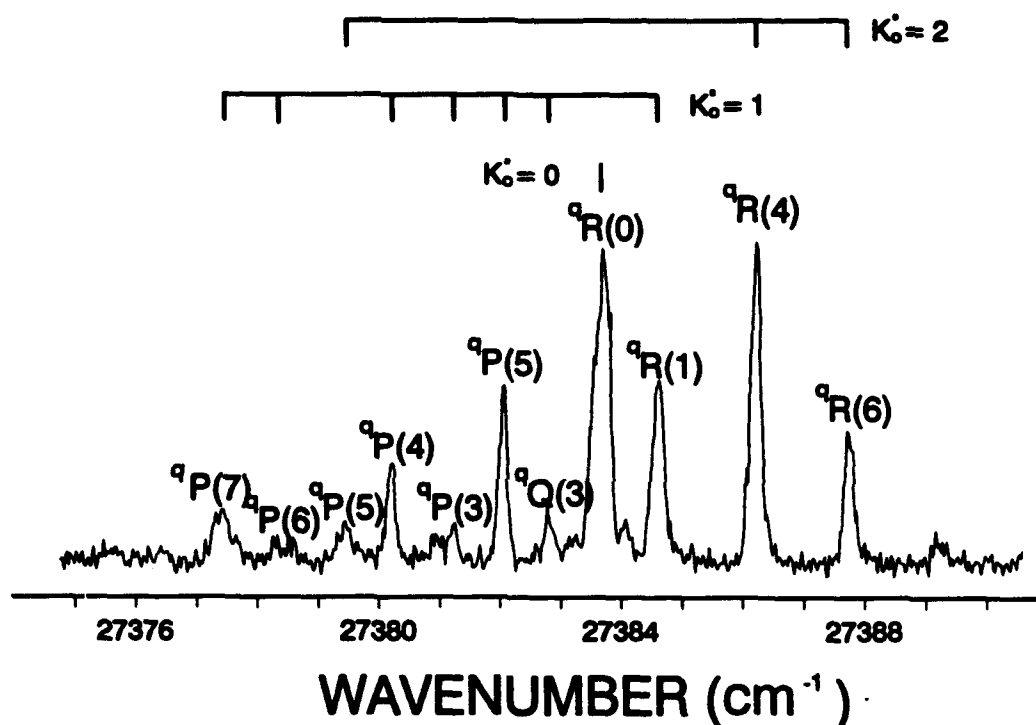


Figure 11: High resolution (0.07 cm<sup>-1</sup>) rotationally-resolved laser excitation spectrum of the  $\tilde{A} \leftarrow \tilde{X}$  band ( $\nu_0 = 27383.3$  cm<sup>-1</sup>) of jet-cooled i-C<sub>3</sub>H<sub>7</sub>O. The photolysis beam was a KrF laser (@248 nm) with an average energy of about 100 mJ/pulse. An excimer-pumped tunable laser with dye BPBD was used to generate a probe beam of about 1 mJ/pulse to record the spectrum.

TABLE 8.

Rotational Transition Frequencies of the ( $\tilde{A}$  -  $\tilde{X}$ ) Band ( $\nu_0=27383.3 \text{ cm}^{-1}$ ) of  
Isopropoxy (i-C<sub>3</sub>H<sub>7</sub>O) with Corresponding Oblate Quantum Number Assignments

J''	K''	J'	K'	Wavenumber (cm <sup>-1</sup> )	Obs-Cal	Transition
0	0	1	0	27383.77	-0.194	<sup>q</sup> R(0)
7	1	6	1	27377.45	-0.041	<sup>q</sup> P(7)
6	1	5	1	27378.33	0.018	<sup>q</sup> P(6)
4	1	3	1	27380.23	-0.035	<sup>q</sup> P(4)
3	1	2	1	27381.24	0.127	<sup>q</sup> P(3)
5	1	5	1	27382.05	-0.028	<sup>q</sup> P(5)
3	1	3	1	27382.81	0.094	<sup>q</sup> Q(3)
1	1	2	1	27384.61	0.069	<sup>q</sup> R(1)
5	2	4	2	27379.52	-0.010	<sup>q</sup> P(5)
4	2	5	2	27386.21	-0.029	<sup>q</sup> R(4)
6	2	7	2	27387.70	0.029	<sup>q</sup> R(6)

**TABLE 9.****Molecular Constants (in  $\text{cm}^{-1}$ ) of the Isopropoxy ( $\text{i-C}_3\text{H}_7\text{O}$ ) Radical**

Constant	$0^0_0$ (Ref. 18) <sup>a</sup>	Band at 27383.3 $\text{cm}^{-1}$
A''	0.273	0.389
B''	0.262	0.323
C''	0.243	0.276
A'	0.254	0.377
B'	0.226	0.308
C'	0.226	0.254
$\nu_0$	27167.1	27383.3

<sup>a</sup> Rotational constants obtained by a fit we performed on the  $0^0_0$  band transitions reported in Ref. 18.

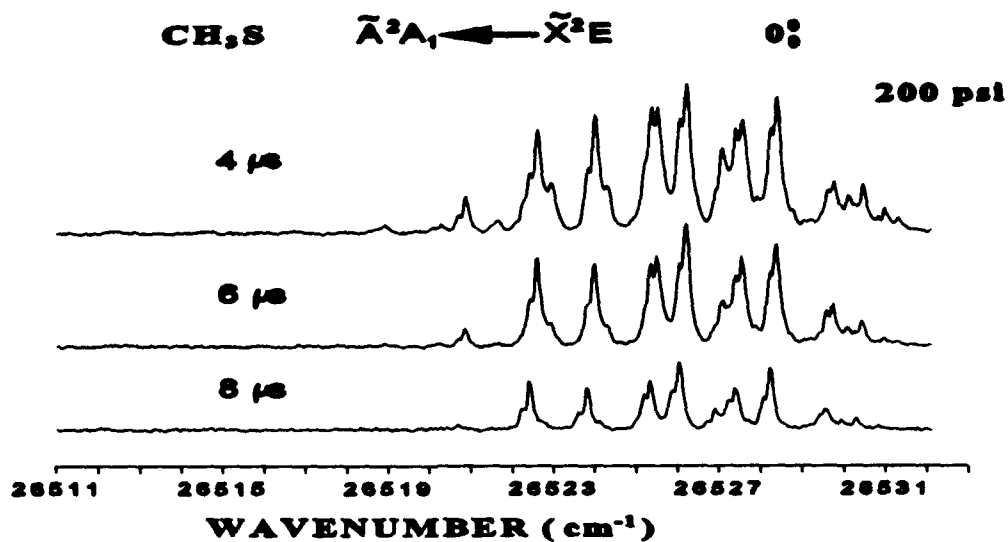


Figure 12. Laser excitation scans showing the 26511-26533  $\text{cm}^{-1}$  spectral region for  $\text{CH}_3\text{S}$  obtained with 200 psi helium backing pressure for three separate time delays of 4  $\mu\text{s}$ , 6  $\mu\text{s}$ , and 8  $\mu\text{s}$ , respectively, between the photolysis and probe lasers.

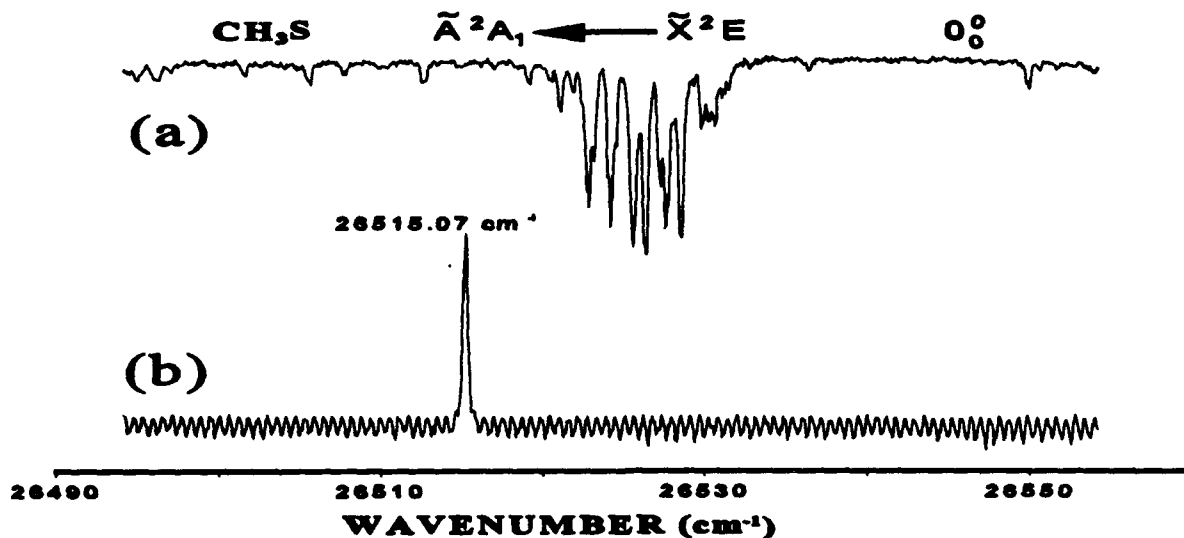


Figure 13. (a) High resolution ( $0.07 \text{ cm}^{-1}$ ) LIF excitation spectrum of the A-X  $0_0$  band of jet-cooled  $\text{CH}_3\text{S}$ . A backing pressure of 200 psi for the helium and  $(\text{CH}_3)_2\text{S}_2$  mixture was maintained behind the pulsed nozzle. (b) A trace showing the optogalvanic neon transition at  $26515.07 \text{ cm}^{-1}$  and simultaneously recorded etalon fringes.

delays and the concomitant enhancement in spectral resolution.

A high resolution ( $0.07\text{ cm}^{-1}$ ) excitation spectrum of the  $\tilde{A}-\tilde{X}\ 0_0^0$  band of jet-cooled  $\text{CH}_3\text{S}$  is shown as an upper trace in Fig. 13(a). The dye Ex 376 was used in the Nd:YAG-pumped tunable dye laser system to generate the requisite wavelength range for recording the  $0_0^0$  LIF spectrum. To be able to perform a reliable detailed analysis of the rotationally-resolved spectra of  $\text{CH}_3\text{S}$ , the dye laser frequency needed to be calibrated precisely. Optogalvanic (OG) transitions of neon and argon, together with simultaneously recorded etalon fringes as shown in Fig. 12(b), allowed accurate calibration of the tunable dye laser frequency.

Analysis of the rotational structure<sup>20</sup> of the  $\tilde{A}\ ^2A_1 - \tilde{X}\ ^2E$  band system for  $\text{CH}_3\text{S}$ , for example, yield  $\nu_0=26398.56\text{ cm}^{-1}$ ,  $A'=5.33\text{ cm}^{-1}$ ,  $B'=0.35\text{ cm}^{-1}$  for the  $0_0^0$  band, and these constants are shown in Table 10, along with similar parameters for  $3_1^0$ .

Wavelength-resolved emission spectra of the  $\tilde{A}-\tilde{X}$  bands of  $\text{CH}_3\text{S}$  obtained with  $0.3\text{ nm}$  resolution have provided ground state vibrational frequencies to within an experimental uncertainty of  $25\text{ cm}^{-1}$ . Figure 14 shows a typical dispersed fluorescence spectrum for  $\text{CH}_3\text{S}$  obtained by pumping the  $0_0^0$  band. Two series of  $\nu_3$  progressions<sup>21,22</sup> are clearly visible corresponding to the  $\tilde{A}\ ^2A_1 \rightarrow \tilde{X}\ ^2E_{3/2}$  and  $\tilde{A}\ ^2A_1 \rightarrow \tilde{X}\ ^2E_{1/2}$  transitions, respectively. The separation between the  $\tilde{X}\ ^2E_{3/2}$  and the  $\tilde{X}\ ^2E_{1/2}$  states gives an accurate value of ( $-266\text{ cm}^{-1}$ ) for the spin-orbit splitting of the  $\text{CH}_3\text{S}$  ground electronic state. In addition to the independent  $\nu_3$  progression in Fig. 14, two other  $\nu_3$  progressions are clearly visible; one in combination with  $\nu_2$ , and the other in association with  $2\nu_2$ . A detailed vibrational analysis of the dispersed fluorescence data for  $\text{CH}_3\text{S}$  has provided the following values for certain fundamental vibrations in the ground state:  $\nu_2''=1330\text{ cm}^{-1}$ ,  $\nu_3''=741\text{ cm}^{-1}$  and  $\nu_6''=608\text{ cm}^{-1}$ . Table 11 summarizes the vibrational intervals observed in dispersed fluorescence involving the  $\tilde{X}\ ^2E$  state of  $\text{CH}_3\text{S}$ .

Analogous to  $\text{C}_2\text{H}_5\text{O}$ , the ethylthio ( $\text{C}_2\text{H}_5\text{S}$ ) radical is a prolate symmetric top molecule ( $k_d \geq 0.80$ ). Figure 15 shows a rotationally-resolved spectrum of the  $\tilde{A}-\tilde{X}$  band ( $\nu_0=25103.9\text{ cm}^{-1}$ ) of jet-cooled  $\text{C}_2\text{H}_5\text{S}$  with separated  $K''$ -manifolds. To the best of our knowledge, such a rotationally-resolved LIF spectrum of  $\text{C}_2\text{H}_5\text{S}$  has been observed and analyzed by us for the *first time*. Table 12 gives the corresponding assigned rotational transitions and Table 13 indicates the rotational parameters obtained from the least-squares fit.

The isopropylthio ( $i\text{-C}_3\text{H}_7\text{S}$ ) radical (akin to  $i\text{-C}_3\text{H}_7\text{O}$ ) is an oblate symmetric top molecule ( $k_d \geq 0.73$ ). A rotationally-resolved excitation spectrum of the  $\tilde{A}-\tilde{X}$  band ( $\nu_0=24773.7\text{ cm}^{-1}$ ) of jet-cooled  $i\text{-C}_3\text{H}_7\text{S}$  has also been recorded and analyzed by us for the *first time*. Figure 16 shows the rotational structure associated with the  $K''=0$  and  $1$  manifolds to be better resolved than those corresponding to  $K''=2$  and  $3$ , as is to be expected for "cold"  $i\text{-C}_3\text{H}_7\text{S}$  radicals. The assigned transitions using oblate quantum numbers are given in Table 14, while Table 13 summarizes the rotational parameters obtained from the least-squares fit for  $i\text{-C}_3\text{H}_7\text{S}$  and compares them with those for  $\text{CH}_3\text{S}$  and  $\text{C}_2\text{H}_5\text{S}$ .

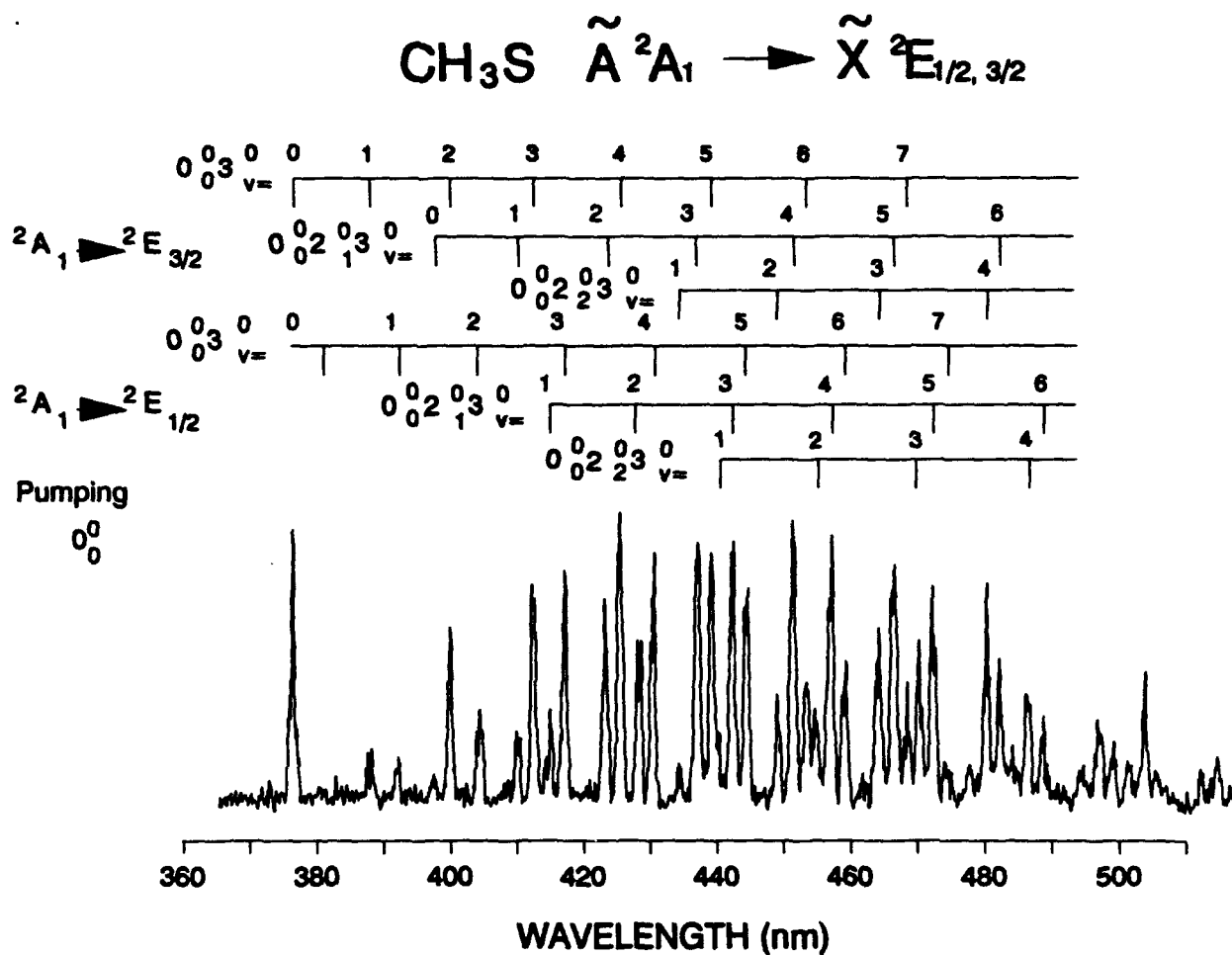


Figure 14. Laser-excited wavelength-resolved emission spectrum of  $\text{CH}_3\text{S}$  observed when the  $0_0^0$  band was pumped. Two series of progressions were seen and correspond to  $\tilde{\text{A}}^2\text{A}_1 - \tilde{\text{X}}^2\text{E}_{3/2}$  and  $\tilde{\text{A}}^2\text{A}_1 - \tilde{\text{X}}^2\text{E}_{1/2}$  transitions, respectively.

TABLE 10.

Band Origins & Upper State ( $\tilde{A}^2A_1$ ) Molecular Constants (in  $\text{cm}^{-1}$ ) for  $\text{CH}_3\text{S}$  Radical

Band	$0^0_0$	$3^1_0$
Parameter	Value	Value
$A'$	5.3256	5.4277
$B'$	0.3452	0.3407
$\nu_0$	26398.56	26798.44
$D'_N$	$6.372 \times 10^{-07} \text{ b}$	$6.372 \times 10^{-07} \text{ b}$
$D'_{NK}$	$8.456 \times 10^{-06} \text{ b}$	$8.456 \times 10^{-06} \text{ b}$
$D'_K$	$8.873 \times 10^{-05} \text{ b}$	$8.873 \times 10^{-05} \text{ b}$

Ground State ( $\tilde{X}^2E$ ) Molecular Constants (in  $\text{cm}^{-1}$ ) for  $\text{CH}_3\text{S}$  Radical

$A'$	5.6800	$\eta_e \xi_t$	$1.51 \times 10^{-05}$	$D'_a$	$6.372 \times 10^{-07} \text{ b}$
$B'$	0.4495813	$\epsilon_{2a}$	-0.13 <sup>a</sup>	$D'_{ak}$	$8.456 \times 10^{-06} \text{ b}$
$A' \xi_t$	3.523	$h_1$	$1.98 \times 10^{-03}$	$D'_k$	$8.873 \times 10^{-05} \text{ b}$
$\eta_k \xi_t$	$7.140 \times 10^{-03}$	$h_{1N}$	0.0	$\epsilon_1$	$-7.906 \times 10^{-03}$
$\epsilon_{aa}$	-3.809	$h_{1K}$	$-7.40 \times 10^{-05}$		
$\epsilon_{bc}$	-0.2583	$h_2$	$2.16 \times 10^{-02}$		
$a \xi_e d$	$-2.555 \times 10^{02}$	$h_{2N}$	$4.19 \times 10^{-07}$		
$a_D \xi_e d$	$-2.81 \times 10^{-03}$	$h_{2K}$	$-1.15 \times 10^{-04}$		

<sup>a</sup>  $\epsilon_{2b} = \epsilon_{2a} \times B'/A'$ <sup>b</sup> also fixed for upper state.

TABLE 11.

Vibrational Assignments of the Intervals Observed in Dispersed Fluorescence of  $\text{CH}_3\text{S } \tilde{X}^2\text{E}$ . The numbers listed are differences between the pump frequency and the corresponding emission frequencies (in  $\text{cm}^{-1}$ ).

$\tilde{A}^2A_1-\tilde{X}^2E_{3/2}$	$\tilde{A}^2A_1-\tilde{X}^2E_{1/2}$	Assignment	$\tilde{A}^2A_1-\tilde{X}^2E_{3/2}$	$\tilde{A}^2A_1-\tilde{X}^2E_{1/2}$	Assignment
0	266		3349	3618	$2\nu_2+\nu_3$
608	875	$\nu_6$	3472	3724	$\nu_2+3\nu_3$
741	1002	$\nu_3$	3550	3823	$5\nu_3$
1330	1596	$\nu_2$	4055	4318	$2\nu_2+2\nu_3$
1461	1726	$2\nu_3$	4157	4422	$\nu_2+4\nu_3$
1919		$\nu_2+\nu_6$	4240	4498	$6\nu_3$
2048	2318	$\nu_2+\nu_3$	4742	5009	$2\nu_2+3\nu_3$
2174	2433	$3\nu_3$	4835	5082	$\nu_2+5\nu_3$
2633	2907	$2\nu_2$	4932	5169	$7\nu_3$
2764	3029	$\nu_2+2\nu_3$	5427	5674	$2\nu_2+4\nu_3$
2866	3127	$4\nu_3$	5530	5774	$\nu_2+6\nu_3$



**(C<sub>2</sub>H<sub>5</sub>S)     $\tilde{A} \longleftarrow \tilde{X}$  Band at 25103.9 cm<sup>-1</sup>**

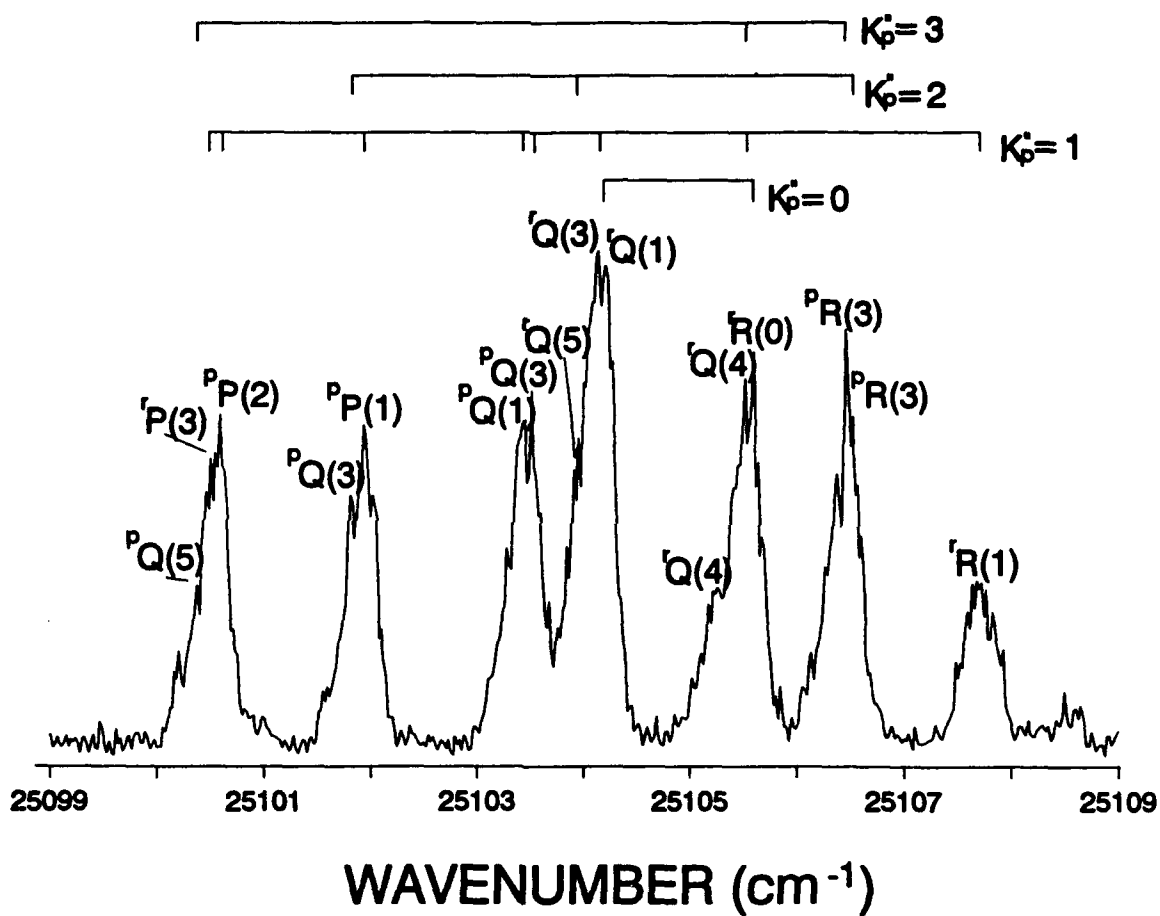


**Figure 15:** High resolution ( $0.07\text{ cm}^{-1}$ ) rotationally-resolved laser excitation spectrum of the  $\tilde{A}-\tilde{X}$  band ( $\nu_0 = 25103.9\text{ cm}^{-1}$ ) of jet-cooled  $\text{C}_2\text{H}_5\text{ S}$ . The photolysis beam was a KrF laser (@248 nm) with an average energy of about 150 mJ/pulse. An excimer-pumped tunable laser with dye Ex 398 was used to generate a probe beam of about 2 mJ/pulse to record the spectrum.

TABLE 12.

Rotational Transition Frequencies of the ( $\tilde{A}$  -  $\tilde{X}$ ) Band ( $\nu_e=25103.90$  cm<sup>-1</sup>) of C<sub>2</sub>H<sub>2</sub>S  
with Corresponding Prolate Quantum Number Assignments

J"	K" <sub>p</sub>	J'	K' <sub>p</sub>	Wavenumber (cm <sup>-1</sup> )	Obs-Cal	Transition
1	0	1	1	25104.20	0.040	'Q(1)
0	0	1	1	25105.59	0.011	'R(0)
3	1	2	2	25100.50	0.035	'P(3)
2	1	1	0	25100.58	0.001	'P(2)
1	1	0	0	25101.93	-0.162	'P(1)
1	1	1	0	25103.44	-0.052	'Q(1)
3	1	3	0	25103.50	0.013	'Q(3)
3	1	3	2	25104.13	-0.065	'Q(3)
4	1	4	2	25105.50	-0.008	'Q(4)
1	1	2	2	25107.67	0.197	'R(1)
3	2	3	1	25101.80	0.103	'Q(3)
5	2	5	3	25103.95	-0.038	'Q(5)
3	2	4	1	25106.51	-0.105	'R(3)
5	3	5	2	25100.37	0.080	'Q(5)
4	3	4	4	25105.25	-0.041	'Q(4)
3	3	4	2	25106.45	-0.001	'R(3)

**TABLE 13.**

**Molecular Parameters (in  $\text{cm}^{-1}$ ) of Alkylthio Radicals**

Parameter	$\text{CH}_3\text{S}$ $0^\circ$	$\text{C}_2\text{H}_5\text{S}$ Band at $25103.90 \text{ cm}^{-1}$	$i\text{-C}_3\text{H}_7\text{S}$ Band at $24773.66 \text{ cm}^{-1}$
$A''$	5.680	1.082	0.268
$B''$	0.450	0.728	0.265
$C''$	--	0.580	0.111
$A'$	5.338	0.995	0.268
$B'$	0.348	0.681	0.227
$C'$	--	0.570	0.044
$\nu_s$	26398.41	25103.90	24773.66

# Isopropylthio

(i-C<sub>3</sub>H<sub>7</sub>S)

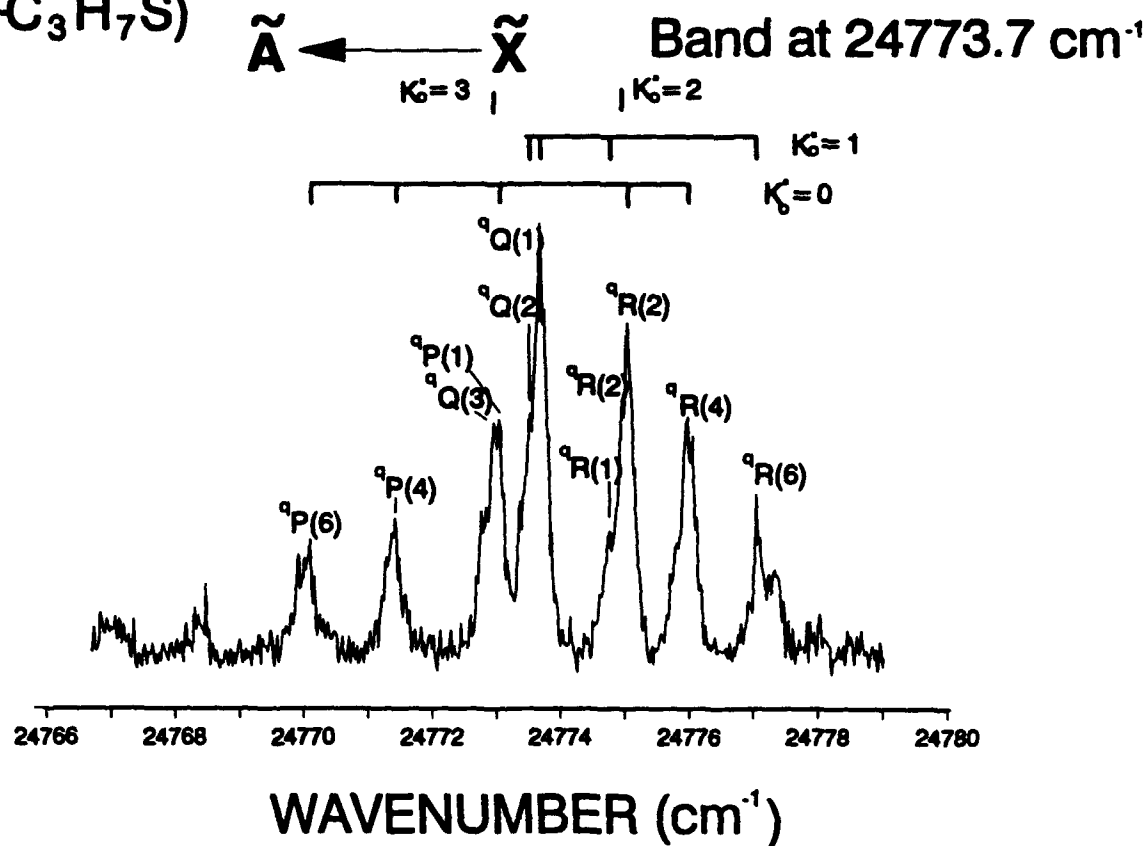


Figure 16: High resolution (0.07 cm<sup>-1</sup>) rotationally-resolved laser excitation spectrum of the  $\tilde{A}-\tilde{X}$  band ( $\nu_0 = 24773.7$  cm<sup>-1</sup>) of jet-cooled i-C<sub>3</sub>H<sub>7</sub>S. The photolysis beam was a KrF laser (@248 nm) with an average energy of about 100 mJ/pulse. An excimer-pumped tunable laser with dye DPS was used to generate a probe beam of about 1.5 mJ/pulse to record the spectrum.

TABLE 14.

Rotational Transition Frequencies of the ( $\tilde{A} - \tilde{X}$ ) Band ( $\nu_0 = 24773.66 \text{ cm}^{-1}$ ) of  $i\text{-C}_3\text{H}_7\text{S}$   
with Corresponding Oblate Quantum Number Assignments

$J''$	$K''_0$	$J'$	$K'_0$	Wavenumber ( $\text{cm}^{-1}$ )	Obs-Cal	Transition
6	0	5	0	24770.08	0.005	$^a\text{P}(6)$
4	0	3	0	24771.39	0.061	$^a\text{P}(4)$
1	0	0	0	24773.01	-0.113	$^a\text{P}(1)$
2	0	3	0	24775.01	-0.050	$^a\text{R}(2)$
4	0	5	0	24775.94	0.001	$^a\text{R}(4)$
2	1	2	1	24773.53	0.102	$^a\text{P}(2)$
1	1	1	1	24773.63	0.083	$^a\text{Q}(1)$
2	1	3	1	24774.74	-0.127	$^a\text{R}(2)$
6	1	7	1	24777.03	0.076	$^a\text{R}(6)$
2	2	3	2	24774.92	0.116	$^a\text{R}(2)$
3	3	3	3	24772.93	-0.057	$^a\text{P}(3)$

## Aromatic Radicals

Laser excitation spectra of the cyclopentadienyl ( $C_5H_5$ ) radical was recorded using the excimer-pumped dye laser system in the range 336-344 nm and employed the dye p-Terphenyl. The LIF spectrum of jet-cooled  $C_5H_5$  obtained in the wavenumber span 29000-29800  $cm^{-1}$  is shown in Fig. 17. The strong spectral feature seen around 29570  $cm^{-1}$  has been identified as the  $\tilde{A}^2A_2 - \tilde{X}^2E_1$   $0^0_0$  band of  $C_5H_5$ .

Various vibronic bands of the "cold" benzyl ( $C_6H_5CH_2$ ) radical belonging to the  $\tilde{A}-\tilde{X}$  electronic system have been recorded in excitation and show A- and B-type transition features. A composite excitation scan showing various vibronic bands of the  $\tilde{A}^2A_2 - \tilde{X}^2B_2$  electronic system of the  $C_6H_5CH_2$  radical is illustrated in Fig. 18. The  $\tilde{A}^2A_2 - \tilde{X}^2B_2$  electronic transition occurs between the ground  $1^2B_2$  state and two closely located excited states, the  $1^2A_2$  and the energetically higher  $2^2B_2$ . In going from low to high frequency, the five featured bands can be identified, respectively as  $0^0_0$ ,  $A^1$ ,  $A^2$ ,  $6a^1_0$  and  $A^3$ .  $A^1$ ,  $A^2$  and  $A^3$  are all A-type transitions that involve a change in dipole moment along the A-axis, while  $6a^1_0$  is a B-type transition. The jet-cooled LIF spectrum of  $C_6H_5CH_2$  as shown in Fig. 18 exhibits the presence of resolved doublet structure for the assigned A- and B-type transitions. The benzyl radical is the prototype of a conjugated benzenoid radical; its asymmetric structure results in challenging complexities in the recorded LIF spectrum.

Several well-resolved vibronic bands of jet-cooled phenyl ( $C_6H_5$ ) radical were found using ArF photolysis of either chlorobenzene ( $C_6H_5Cl$ ) or bromobenzene ( $C_6H_5Br$ ) and the excimer-pumped dye laser with various dyes (having a typical average energy of 1-2 mJ per pulse). Both precursors gave rise to identical spectra for the fragment  $C_6H_5$ . Extensive LIF spectra of  $C_6H_5$  have been recorded in the 19,000-24,200  $cm^{-1}$  region. Illustrative LIF spectra of phenyl are shown in Fig. 19 in the range 22900-22970  $cm^{-1}$ . To the best of our knowledge, the LIF spectra for the jet-cooled phenyl radical have been recorded by us for the *first time*. The origin band was located around 19409  $cm^{-1}$ . Our scans reveal a complicated spectrum with five different types of recognizable band structures: (a) Doublets 10  $cm^{-1}$  wide at 136, 121 and 105  $cm^{-1}$  intervals; (b) Doublets 7  $cm^{-1}$  wide at 316, 266 and 210  $cm^{-1}$  intervals; (c) Triplets (with 1.5  $cm^{-1}$  separation between peaks) at an interval of 424  $cm^{-1}$ ; (d) Doublets 2  $cm^{-1}$  wide at 159 and 148  $cm^{-1}$  intervals; and (v) Sextets at 1738, 1721, 1715, 98, 80, 60, 58 and 38  $cm^{-1}$  intervals. Our analysis indicates the electronic system for the observed transitions to be either  $^2A_2 - \tilde{X}^2A_1$  or  $^2B_1 - \tilde{X}^2A_1$ .

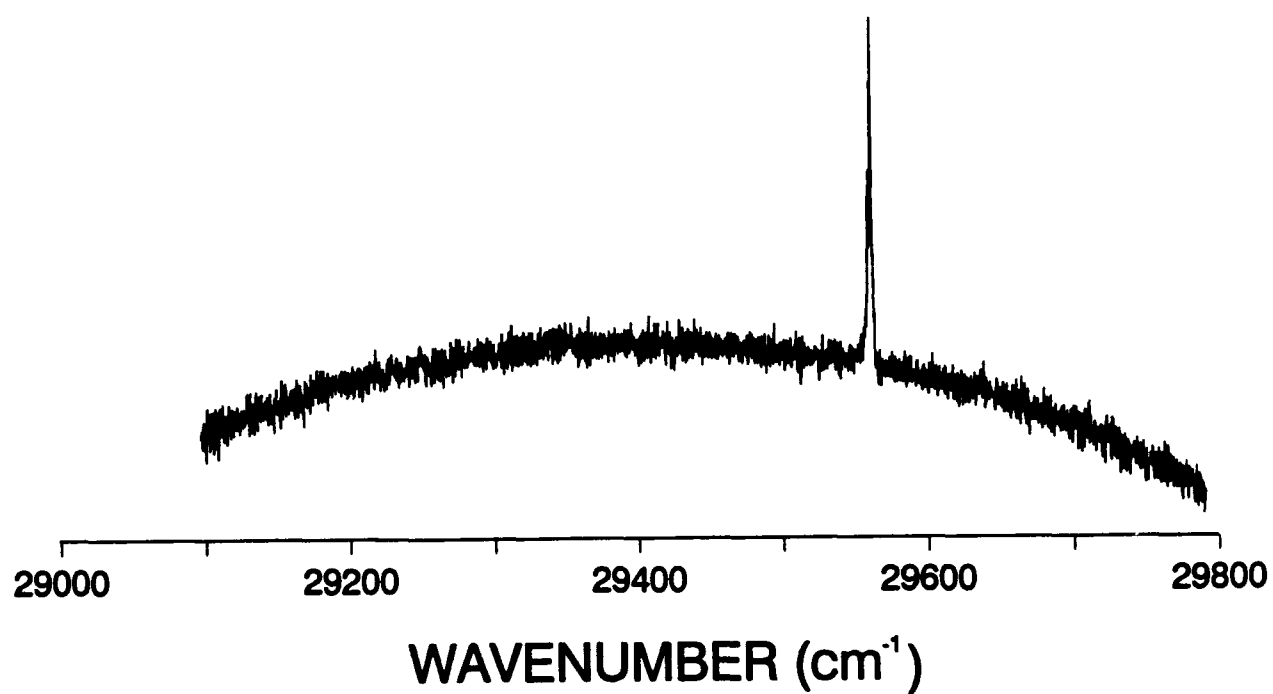
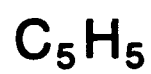
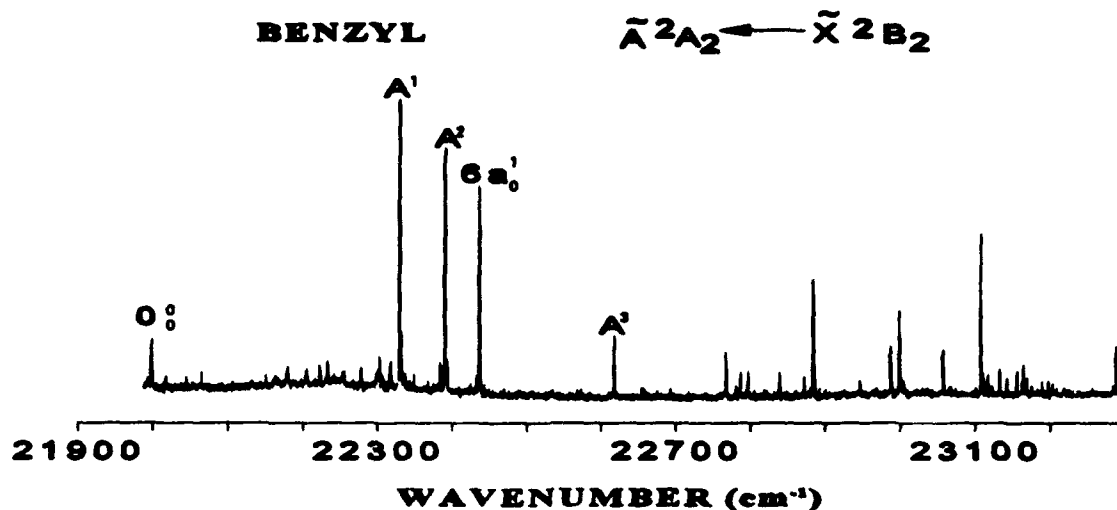
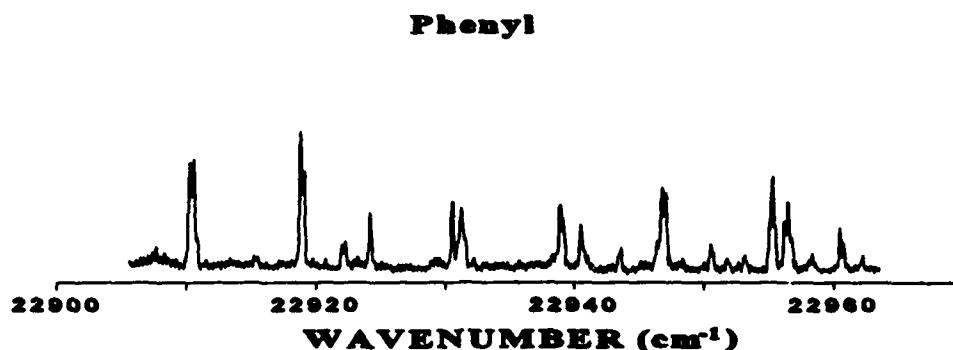


Figure 17. LIF excitation spectrum of the  $\tilde{A}^2A_2^+ - \tilde{X}^2E_1^+ 0_0^0$  band of  $C_5H_5$ .



**Figure 18.** Laser excitation spectrum of benzyl showing various vibronic bands belonging to the  $\tilde{A}^2A_2 - \tilde{X}^2B_2$  electronic system. A backing pressure of 200 psi helium was maintained behind the nozzle and there was a time delay of 8  $\mu$ s between the photolysis and probe lasers.



**Figure 19.** Laser excitation scan showing the 22900-22980 cm<sup>-1</sup> spectral region for phenyl obtained with 200 psi helium backing pressure and a time delay of 6.5  $\mu$ s between the photolysis and probe lasers. The excimer-pumped dye laser with C440 dye had an average energy of 2 mJ per pulse.



#### 4. References

1. S.C. Foster and T.A. Miller, *J. Phys. Chem.* **93**, 5986 (1989).
2. T.A. Miller, *Science* **223**, 545 (1984).
3. S.C. Foster, P. Misra, T.-Y.D. Lin, C.P. Damo, C.C. Carter, and T.A. Miller, *J. Phys. Chem.* **92**, 5914 (1988); X. Liu, C.P. Damo, T.-Y.D. Lin, S.C. Foster, P. Misra L. Yu, and T.A. Miller, *J. Phys. Chem.* **93**, 2266 (1989).
4. S.C. Foster, R.A. Kennedy, and T.A. Miller, "Laser Spectroscopy of Chemical Intermediates in Supersonic Free Jet Expansions," in *Frontiers of Laser Spectroscopy of Gases*, A.C.P. Alves et al. (eds.), Kluwer Academic Publishers, pp. 421-449, 1988.
5. T. Momose, Y. Endo, E. Hirota, and T. Shida, *J. Chem. Phys.* **88**, 5338 (1988).
6. S.-Y. Chiang and Y.P. Lee, *J. Chem. Phys.* **95**, 66 (1991).
7. G. Porter and B. Ward, *Proc. Roy. Soc. (Lond)* **A287**, 457 (1965).
8. L.J. Radziemski, R.W. Solarz, and J.A. Paisner (eds.), *Laser Spectroscopy and Its Applications*, Marcel Dekker, New York, 1987.
9. S. Hatakeyama and H. Akimoto, *J. Phys. Chem.* **87**, 2387 (1983).
10. A.H. Blatt, ed., *Organic Syntheses*, Collective Vol. 2, Wiley, New York, 1943.; E.C. Horing, ed., *Organic Syntheses*, Collective Vol. 3, Wiley, New York, 1955.
11. G. Porter and B. Ward, *J. Chim. Phys.* **61**, 1517 (1974).
12. N. Ikeda, N. Nakashima, and K. Yoshihara, *J. Am. Chem. Soc.* **107**, 3381 (1985).
13. S. Gerstenkorn and P. Luc, "Atlas du Spectra d'absorption de la Molecule d'Iode, Paris: Centre National de la Recherche Scientifique, 1978.
14. J.M. Brown, *Molec. Phys.* **20**, 817 (1971).
15. G. Herzberg, *Electronic Spectra and Electronic Structure of Polyatomic Molecules*, Van-Nostrand-Reinhold, New York, 1966.
16. P. Misra, X. Zhu, and A.H. Nur, *Spectrosc. Lett.* **25**, 639 (1992); P. Misra and X. Zhu, *Spectrosc. Lett.* **26**, 389 (1993).

17. P. Misra, X. Zhu, C.-Y. Hsueh, and J.B. Halpern, *Chem. Phys.* **178**, 377 (1993).
18. S.C. Foster, Y.-C. Hsu, C.P. Damo, X. Liu, C.-Y. Kung, and T.A. Miller, *J. Phys. Chem.* **90**, 6766 (1986).
19. X.Q. Tan, J.M. Williamson, S.C. Foster, and T.A. Miller, *J. Phys. Chem.* **97**, 9311 (1993).
20. Y.-C. Hsu, X. Liu, and T.A. Miller, *J. Chem. Phys.* **90**, 8652 (1989).
21. P. Misra, X. Zhu, M.M. Kamal, A.H. Nur, and H. Bryant, *Proc. International Conference on Laser '93* (1994, in press).
22. M. Suzuki, G. Inoue, and H. Akimoto, *J. Chem. Phys.* **81**, 5405 (1984).

**Research Presentations and Publications Acknowledging Financial Support from Wright-Patterson AFB (Grant # F33615-90-C-2038):**

1. "Laser Spectroscopy of the Hydroxyl and Alkoxy Radicals in a Supersonic Jet," P. Misra, X. Zhu, and A.H. Nur, Joint Meeting of the American Physical Society and the American Association of Physics Teachers, Washington, D.C., April 1992, Bull. Am. Phys. Soc. 37 (2), B10 5, 890 (1992).
2. "Laser Excitation Spectroscopy of Jet-Cooled Hydroxyl and Methoxy Radicals in the Overlapping 308-317 nm Spectral Region," Abdullahi H. Nur, Xinming Zhu, and Prabhakar Misra, XXth Informal Conference on Photochemistry, Georgia Institute of Technology, GA, May-June 1992.
3. "Supersonic Jets and Excimer Lasers: A Stable Marriage for the Study of Unstable Free Radicals," Prabhakar Misra, Colloquium, Department of Physics & Astronomy, Howard University, Washington, D.C., February 1993.
4. "Laser Jet Spectroscopy of Methoxy and Methylthio Radicals," Hosie L. Bryant and Prabhakar Misra, Paper 81, Graduate Research Symposium, Howard University, Washington, D.C., April 1993.
5. "High Resolution Laser Induced Fluorescence Spectroscopy of the  $\text{CH}_3\text{O}$  and  $\text{CH}_3\text{S}$  Radicals," Mohammed M. Kamal and Prabhakar Misra, Paper 80, Graduate Research Symposium, Howard University, Washington, D.C., April 1993.
6. "Vibronic and Rotational Analyses of LIF Spectra of  $\text{CH}_3\text{O}$  and  $\text{CH}_3\text{S}$  Radicals," P. Misra, X. Zhu, H. Bryant, A. Nur, and M. Kamal, Joint Meeting of the American Physical Society and the American Association of Physics Teachers, Washington, D.C., April 1993, Bull. Am. Phys. Soc. 38 (2), E11 7, 970 (1993).
7. "Chemiluminescent Studies Involving Collisions of  $\text{CHO}^+$  Ions and  $\text{CH}_4$  Molecules," A. Michael, P. Misra and V. Kushawaha. J. Appl. Spectrosc. 46 (5), 797-799 (1992).
8. "Laser Induced Fluorescence Spectroscopy of the Hydroxyl Radical," Prabhakar Misra, Xinming Zhu, and Abdullahi H. Nur. Spectrosc. Lett. 25 (4), 547-557 (1992).
9. "Rotationally-Resolved Excitation Spectroscopy of the Methoxy Radical in a Supersonic Jet," Prabhakar Misra, Xinming Zhu, and Abdullahi H. Nur. Spectrosc. Lett. 25 (5), 639-649 (1992).

10. "Electronic Emission Due to Collisions Involving Low Energy  $\text{CHO}^+$  and  $\text{H}^+$  Ions and  $\text{CH}_4$  and  $\text{N}_2$  Molecules", A. Michael, P. Misra, A. Farah, and V. Kushawaha. J. Phys. B: At. Mol. Opt. Phys. **25**, 2343-2350 (1992).
11. "Rotationally-Resolved Excitation Spectroscopy of the Alkoxy and Alkylthio Radicals in a Supersonic Jet," Prabhakar Misra, Xinming Zhu, Hosie L. Bryant, and Mohammed M. Kamal, Paper TJ.7, Proc. Fifteenth International Conference on Lasers '92, Houston, TX, 696-701 (1992).
12. "Wavelength-Resolved Emission Spectroscopy of the Alkoxy and Alkylthio Radicals in a Supersonic Jet," Prabhakar Misra, Xinming Zhu, Ching-Yu Hsueh, and Mohammed M. Kamal, Paper TJ.8, Proc. Fifteenth International Conference on Lasers '92, Houston, TX 702-705 (1992).
13. "Laser Excitation Spectroscopy of the Jet-Cooled Methoxy Radical Amidst Hydroxyl Transitions," Prabhakar Misra and Xinming Zhu. Spectrosc. Lett. **26** (2), 389-402 (1993).
14. "Laser Excitation Spectroscopy of Jet-Cooled Alkoxy and Alkylthio Radicals," P. Misra, X. Zhu, H.L. Bryant, R. Pai, A.H. Nur, M.M. Kamal, and S. Alagudu, Paper QTuK48, Proc. CLEO/QELS (Conference on Lasers & Electro-Optics / Quantum Electronics & Laser Science Conference), **12**, 122 (1993).
15. "Laser Excitation and Emission Spectroscopy of the Methoxy Radical in a Supersonic Jet," Prabhakar Misra, Xinming Zhu, Ching-Yu Hsueh, and Joshua B. Halpern. Chemical Physics **178**, 377-385 (1993).
16. "Laser-Induced Fluorescence Spectroscopy of Jet-Cooled Free Radicals," Prabhakar Misra, Xinming Zhu, Mohammed M Kamal, Abdullahi H. Nur, and Hosie L. Bryant, Jr. Proc. International Conference on Lasers '93 (1994, in press).
17. "Rotationally Resolved Spectroscopy of Jet-Cooled Alkoxy and Alkylthio Radicals," Prabhakar Misra, Xinming Zhu, Mohammed M. Kamal, and Rajendra V. Pai, Manuscript in Preparation for Journal of Molecular Spectroscopy (1994).